INAF

ISTITUTO NAZIONALE DI ASTROFISICA
OSSERVATORIO ASTROFISICO DI ARCETRI

UNIVERSITÀ DEGLI STUDI FIRENZE

Lecture V:
The Spectral Energy Distribution of Galaxies
Star Formation Rate, Ionized ISM

Astrophysics of Galaxies 2019-2020

Stefano Zibetti - INAF Osservatorio Astrofisico di Arcetri

Lecture V

Star Formation Rate (SFR)

- SFR= dM*/dt
  - galaxies evolve, and not only passively
- rely on short-lived stars to measure SFR
  - if they are “observed” (directly or indirectly), they must have formed less than Δt time ago

Why short-lived stars trace SFR

$$N_{\overline{stars}} = k \int_{-\infty}^{0} dt\ SFR(t)\, f_{surv}(-t)$$

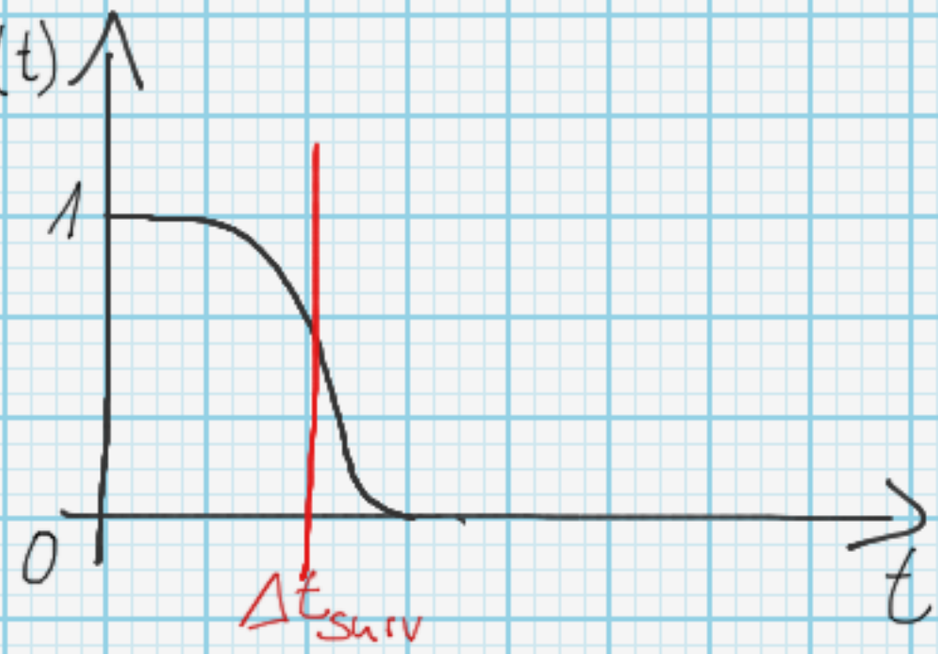

$$N_{\overline{stars}} \simeq k \int_{-\Delta t_{surv}}^{0} dt\ SFR(t) = k \langle SFR(0) \rangle_{\Delta t_{surv}} \Delta t_{surv}$$

$$\Rightarrow N_{\overline{stars}} \propto \langle SFR(0) \rangle_{\Delta t_{surv}}$$

How can we "count" short lived stars?

- Mass-t_{surv} relation

$$t \propto \frac{M}{L} \propto \frac{M}{M^4} \propto M^{-3}$$

- Mass-T_{eff} relation
- ⇒ follow the UV photons!
- t-M* "uncertainty principle": the more "instantaneous" the SFR measurement, the largest the extrapolation in mass

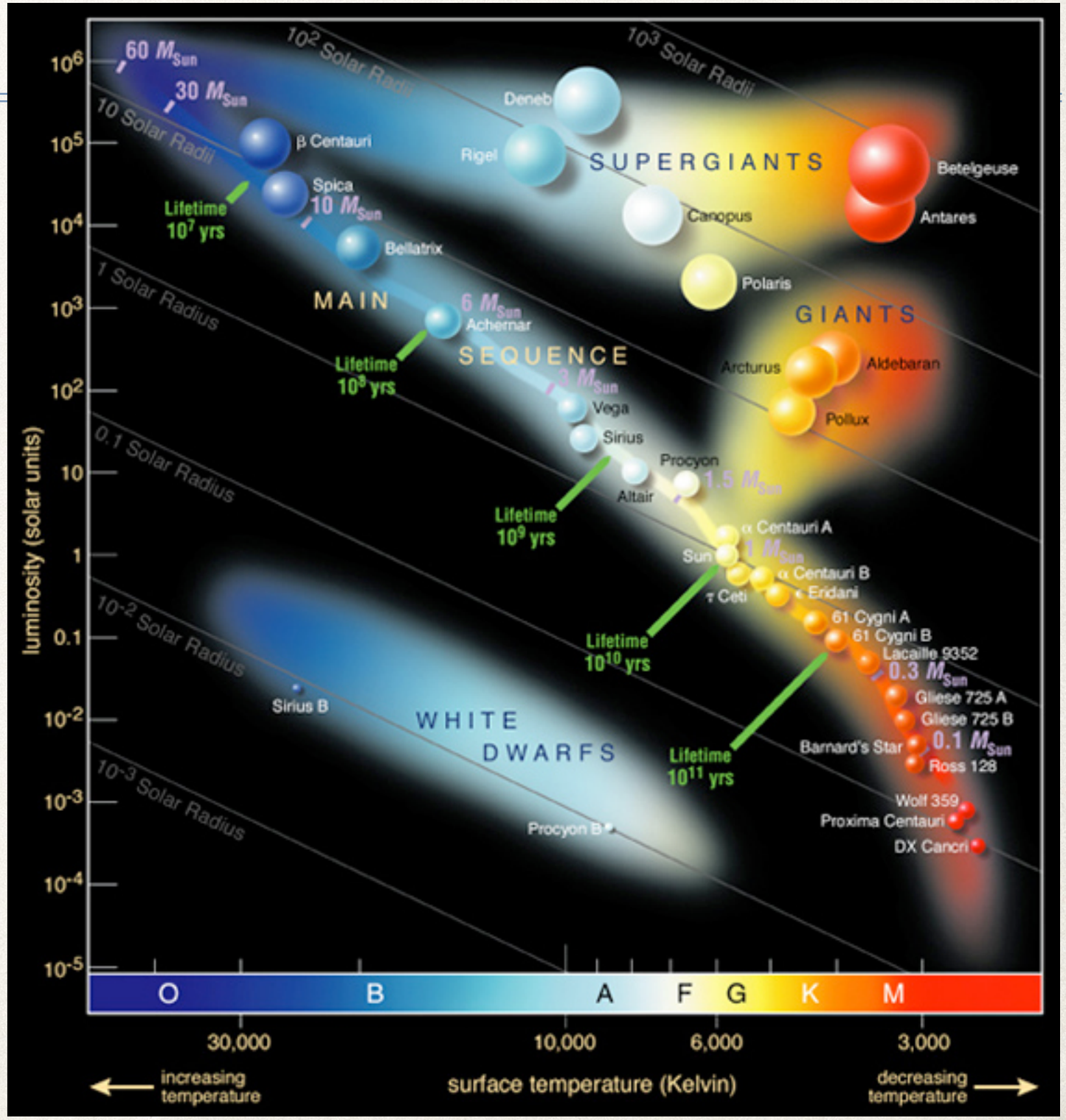

The fate of UV photons

- The highest-energy UV photons (E>13.6 eV, i.e. 912Å) ionize the atoms in the birth clouds of stars, cascade down the recombination ladders
  - Hydrogen series (mainly Balmer, Paschen, Brackett; Lyman is resonant, not optically thin)
  - other nebular lines (e.g. [OII]) are excited by hot free electrons
- Lower energy UV photons escape and produce UV luminosity, possibly attenuated by dust
- All can heat up dust and excite ISM molecular emission (like PAHs)

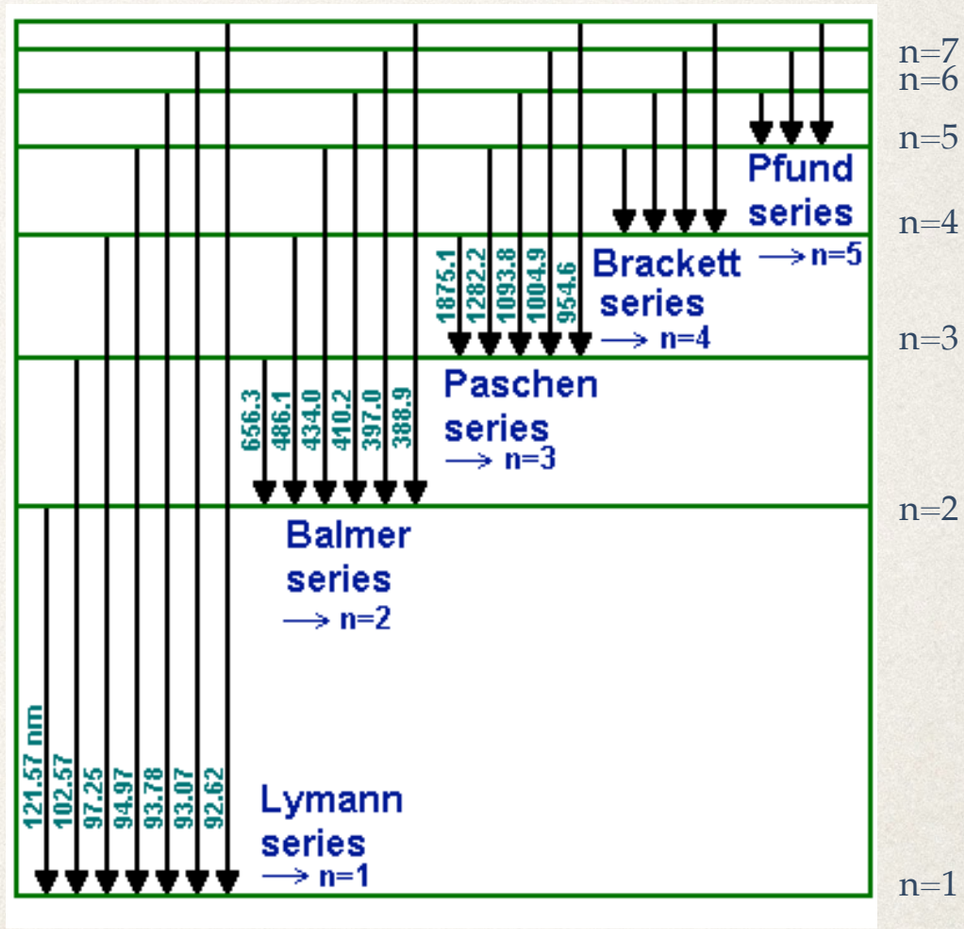

Hydrogen recombination lines

- Ionized ISM is optically thin to non-resonant lines (not so many atoms/ions excited above the ground state), i.e. NOT H Lyα, C IVλ1550, N Vλ1240, Mg IIλ2800
- Intensity of hydrogen recombination lines almost independent of T, ~proportional to the number of recombinations, hence to the number of ionizing photons if equilibrium holds and all ionizing photons absorbed ("case B")
- Dust extinction can be estimated based on recombination line ratios: the theoretical ratio is altered by wavelength dependent extinction; once an extinction curve is assumed, one just needs the extinction ratio at two different λ to get the optical depth
- Intrinsic line luminosity can be derived $\Rightarrow$ ionizing flux
- SPS models provide the conversion from ionizing flux to SFR
- Only stars with M>10$M_\odot$ and life-time <20 Myr contribute significantly:
  - "instantaneous" measurement
  - large uncertainties due to IMF, which is however constrained by EW(Halpha)

Extinction from "Balmer decrement"

$$\frac{L(H\alpha)}{L(H\beta)} \simeq \frac{\alpha^{eff}_{H\alpha}(H^0, T_e)}{\alpha^{eff}_{H\beta}(H^0, T_e)} \approx 3 \quad \text{per } T_e = 10^4 \text{ K}$$

$$\left[\frac{F_\lambda(H\alpha)}{F_\lambda(H\beta)}\right]^{oss} = \left[\frac{F_\lambda(H\alpha)}{F_\lambda(H\beta)}\right]^{em} 10^{(A_{H\beta}-A_{H\alpha})/2.5}$$

$$\left[\frac{F_\lambda(H\alpha)}{F_\lambda(H\beta)}\right]^{oss} \approx 3 \times 10^{A_V[f(H\beta)-f(H\alpha)]/2.5}$$

f(λ) is the assumed extinction curve

A_V is the only left unknown

Recombination lines across the Hubble sequence: a sequence of SFH intensity

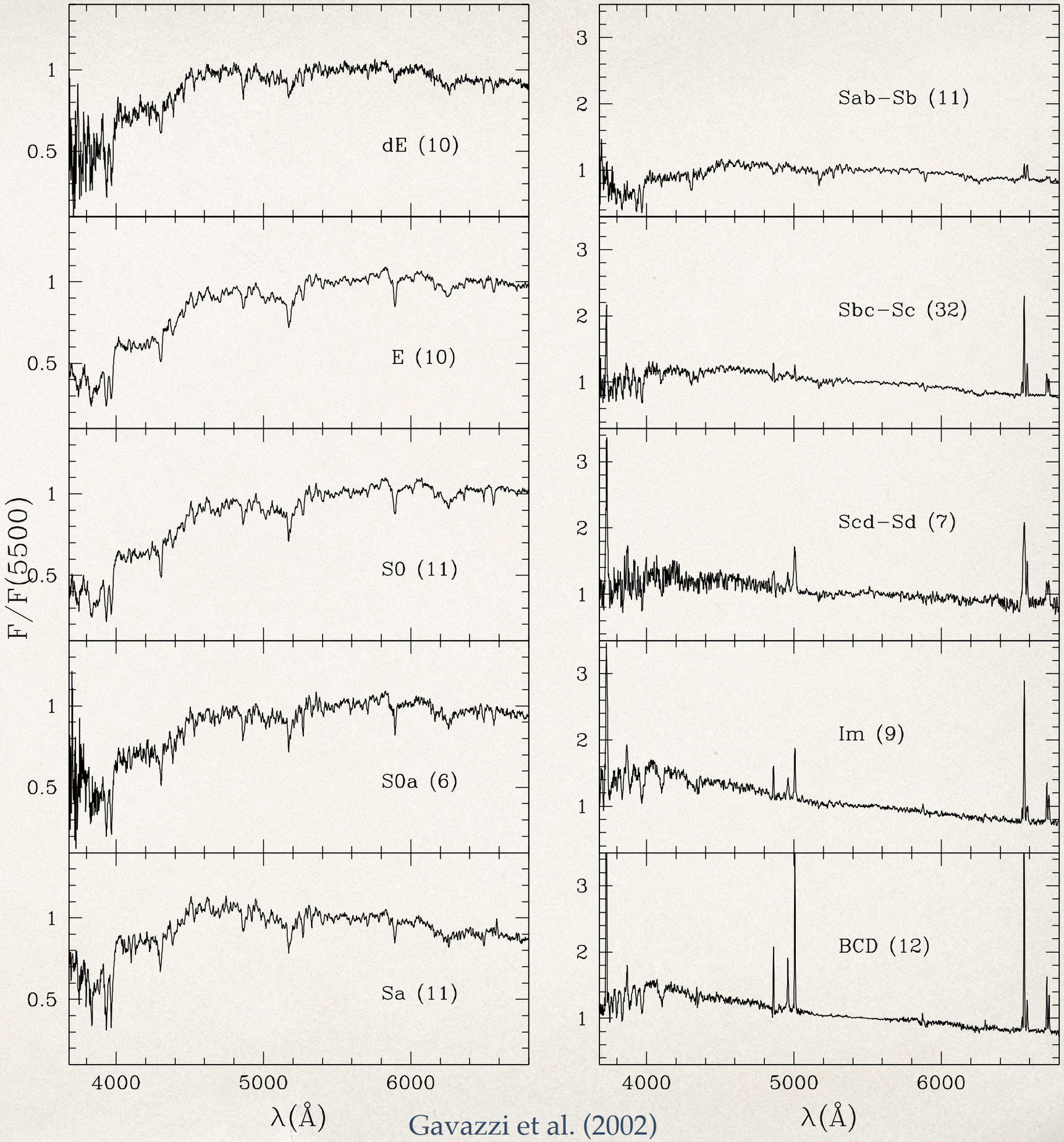

Gavazzi et al. (2002)

The plethora of NIR recombination lines

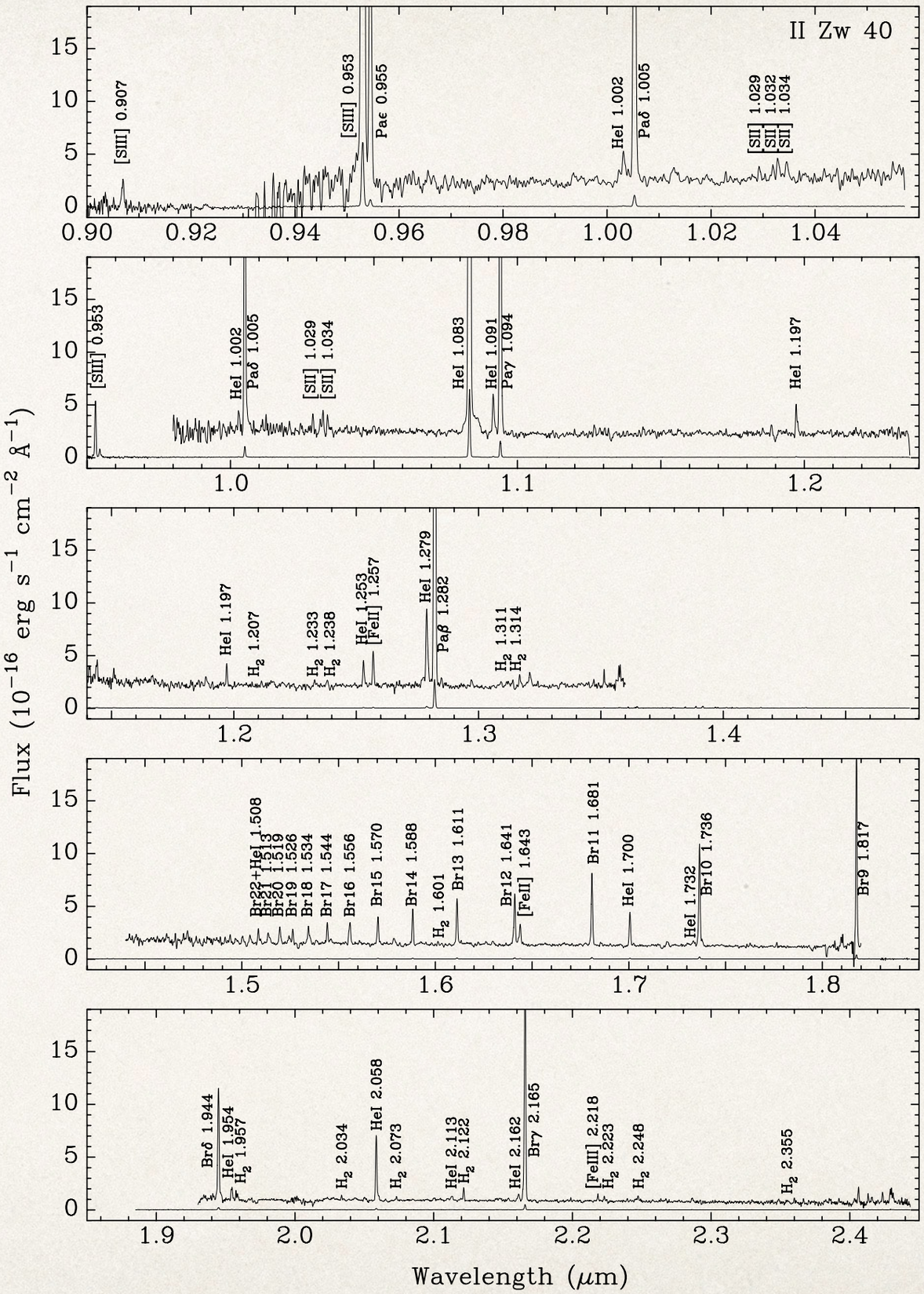

Figure 1. 3.5 m APO/TripleSpec NIR spectrum of II Zw 40 in five orders. In each panel, the noisy regions of the upper spectrum are omitted. They are caused by insufficient sensitivity or strong telluric absorption. The flux scale on the *y*-axis corresponds to the upper spectrum. The lower spectrum is downscaled by a factor of 50 as compared to the upper spectrum. It is shown for the whole wavelength range in each order.

Survey: *sdss* Program: *legacy* Target: *GALAXY*
RA=212.53525, Dec=53.64031, Plate=1324, Fiber=54, MJD=53088
z=0.04283±0.00001 Class=GALAXY STARFORMING
No warnings.

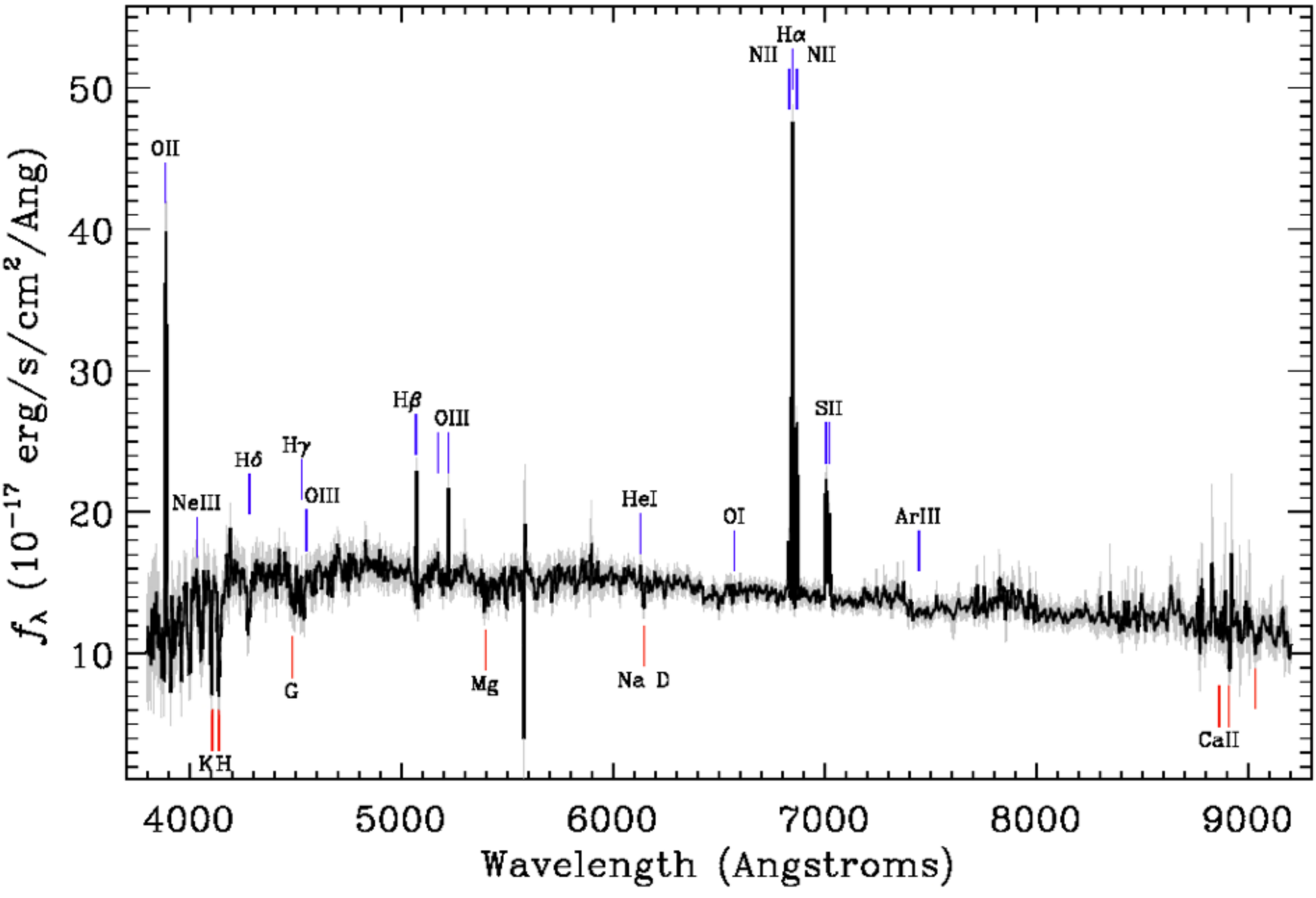

SFR from forbidden lines: [OII]

- very useful to extend to higher z but staying in the optical window

- forbidden lines in general are not directly coupled to ionizing radiation (see next slides), BUT [OII] is well behaved and can be calibrated empirically.

- metal abundance has a relatively small effect on the [OII] calibration, over most of the abundance range of interest ($0.05\ Z_\odot \leq Z \leq 1\ Z_\odot$)

Attenuation

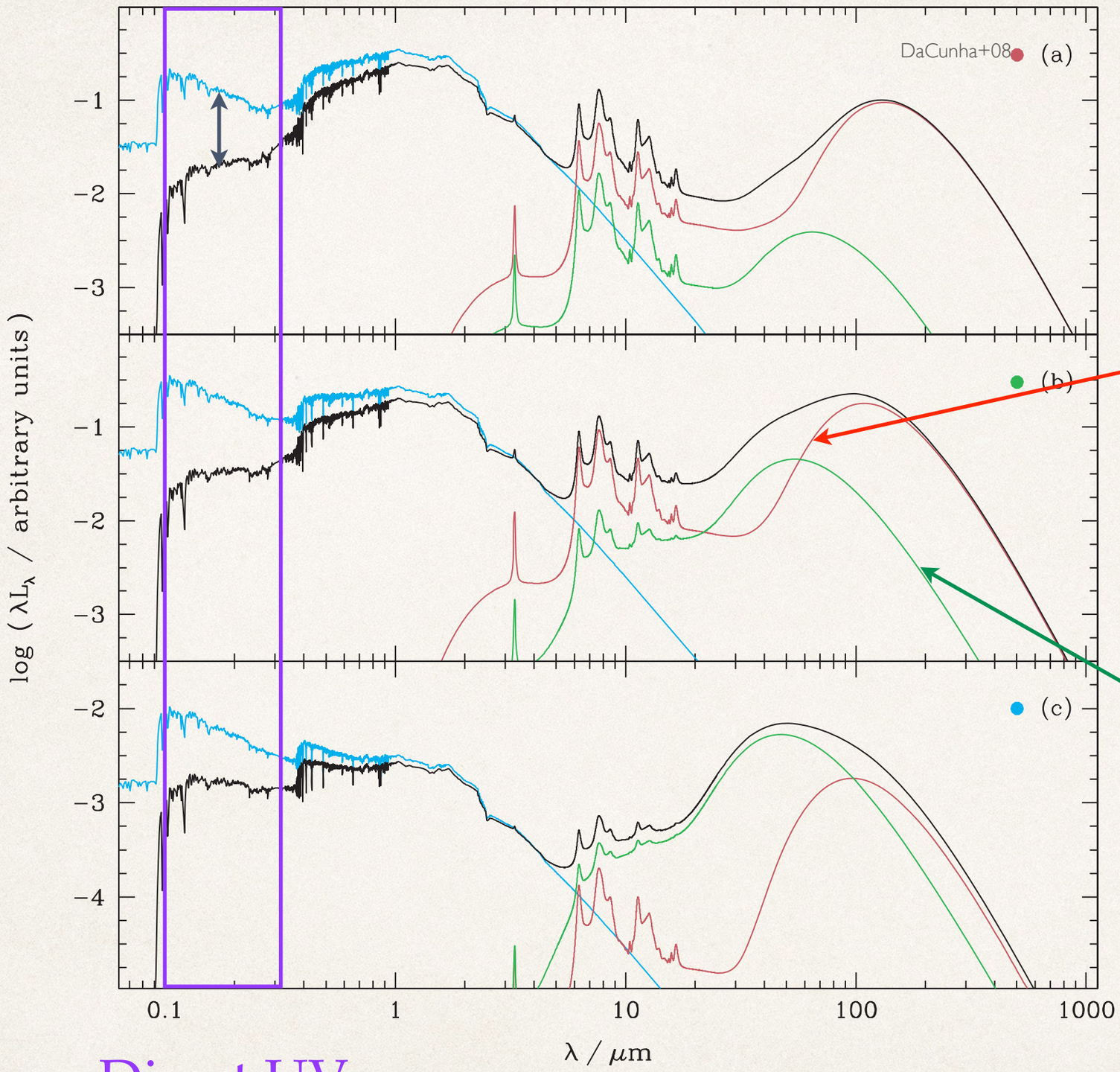

Direct UV
(non-ionizing, λ>912Å)

"Cirrus" component, heated by diffuse ISRF

"Warm" component, directly heated by hot stars

SFR from UV continuum

- Use SPS models assuming
  - IMF
  - SFH: adapt to the galaxy to study
    - typically constant over the time traced by the UV bright stars
    - shorter if considering a starburst
- Integrated spectrum 1500-2500Å dominated by stars $M \gtrsim 5\ M_\odot$
  - timescale ~10^8 yr
  - substantial extrapolation to total mass
- Large sensitivity to dust extinction, typically 0-3 mag, but can be much much more for dusty starburst!
  - β-A_{UV} relation: empirically calibrated via IRX, assuming all IR is re-radiated flux missing from the UV (Meurer, Heckman & Calzetti 1999)

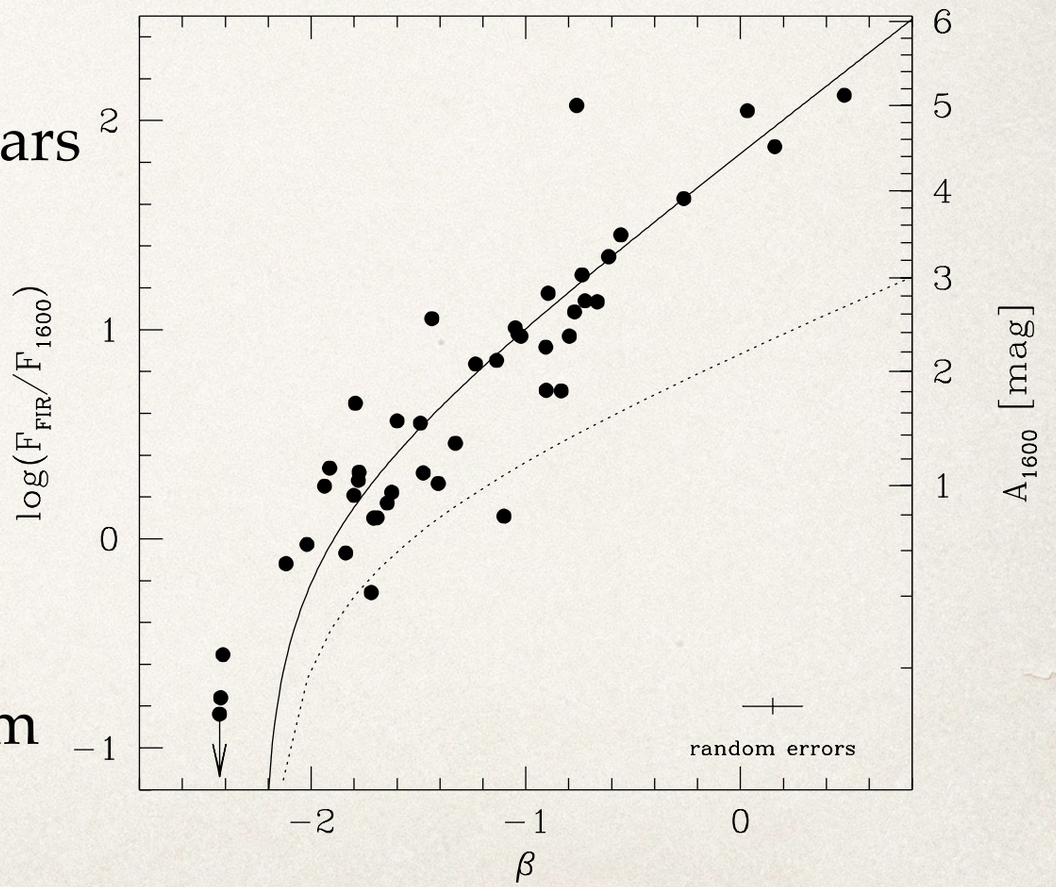

SFR from IR continuum

- Total IR luminosity L_{TIR} is a good proxy for SFR as long as
  - most of the UV photons are absorbed and re-radiated by dust
  - dust heating is predominantly done by young hot stars
    - note that the absorption cross section of dust increases at shorter λ

FIG. 1.—The extinction law $k(\lambda)$ is shown as a function of λ for the Milky Way (*continuous line*), Large Magellanic Cloud (*dot-dashed line*), and Small Magellanic Cloud (*dashed line*). $k(\lambda) = A(\lambda)/E(B-V)_i = 1.086\tau(\lambda)/E(B-V)_i$, where $A(\lambda)$ is the extinction in magnitudes, $\tau(\lambda)$ is the extinction optical depth, and $E(B-V)_i$ is the color excess in B relative to V, $A(V)/E(B-V)_i = 3.1$.

Calzetti, Kinney & Storchi-Bergmann (1994)

Proxies to TIR (and SFR)

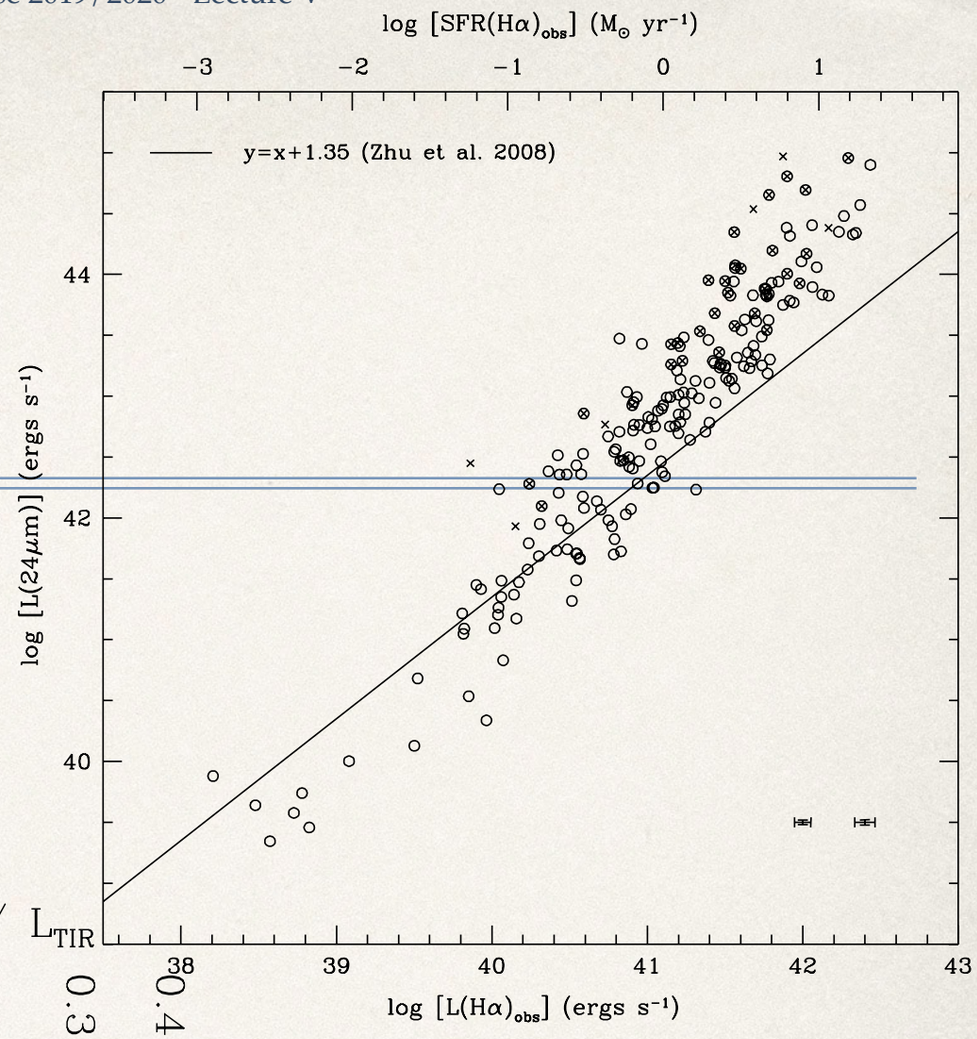

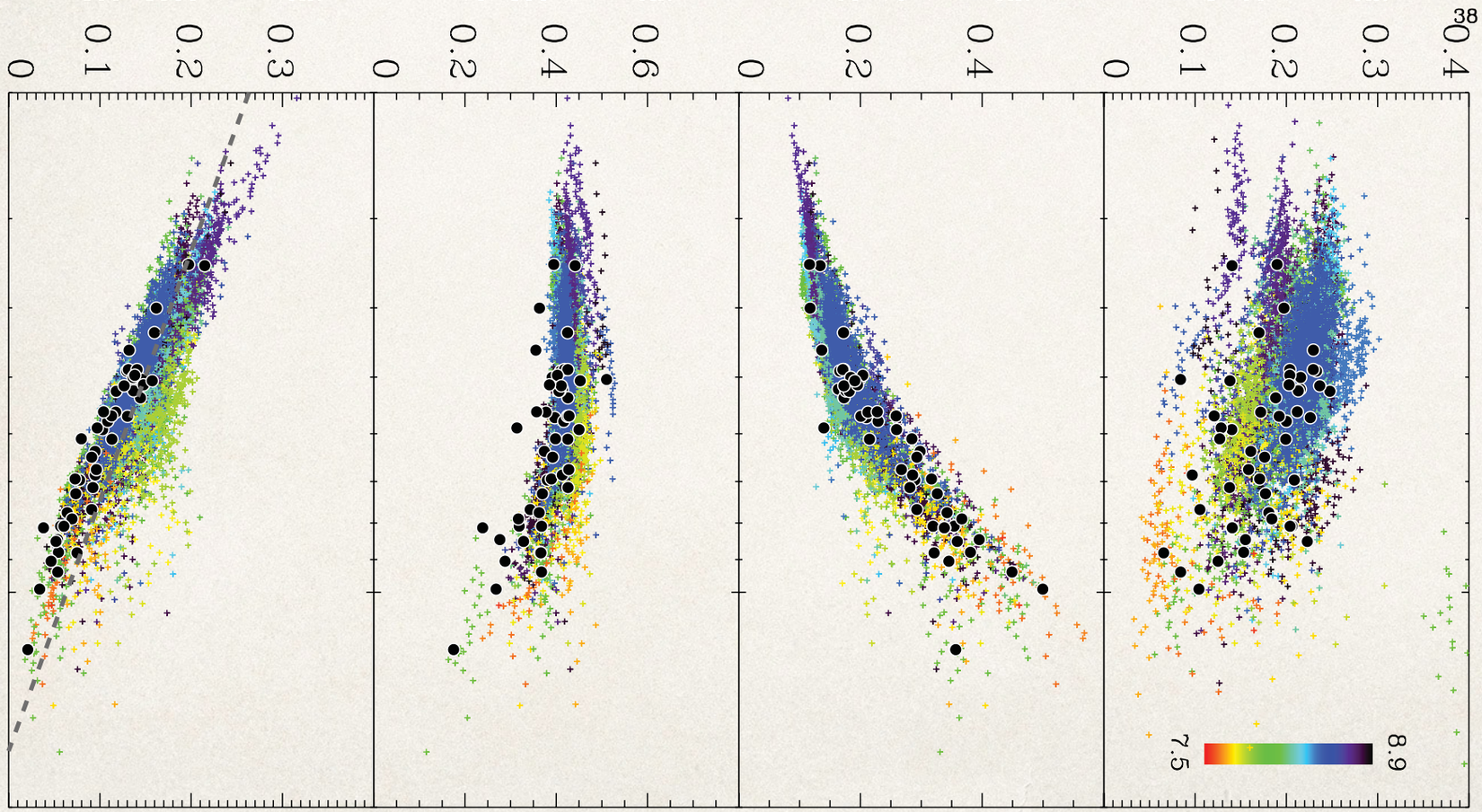

Kennicutt+09

Galametz+13
coded by 12+log(O/H)

Mid IR: PAHs and hot dust

- Dominated by hot dust and PAH emission, excited by soft UV (see e.g. Draine+07)
- PAH luminosity: dependence on metallicity
- 8μm must be decontaminated from stellar continuum

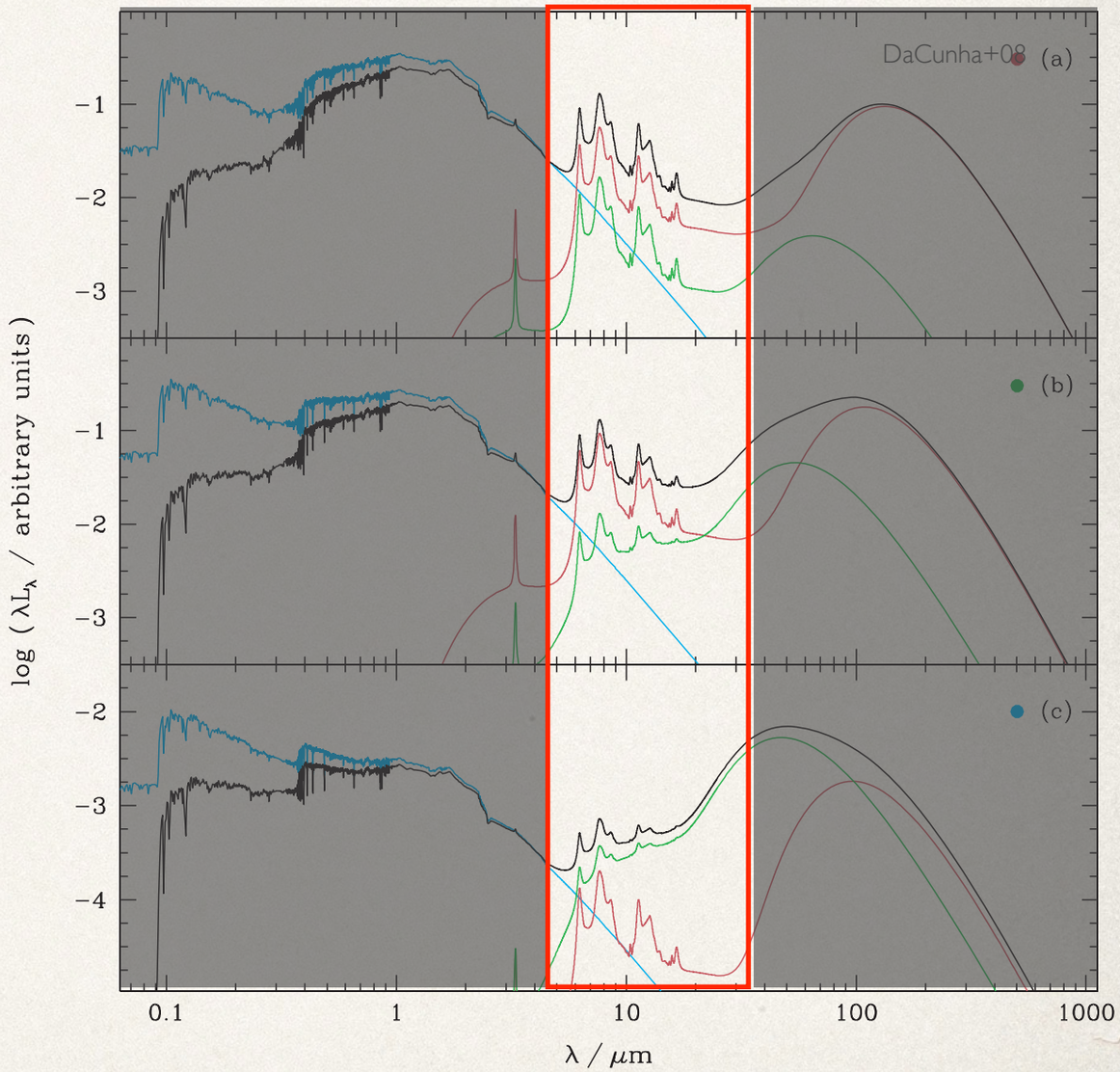

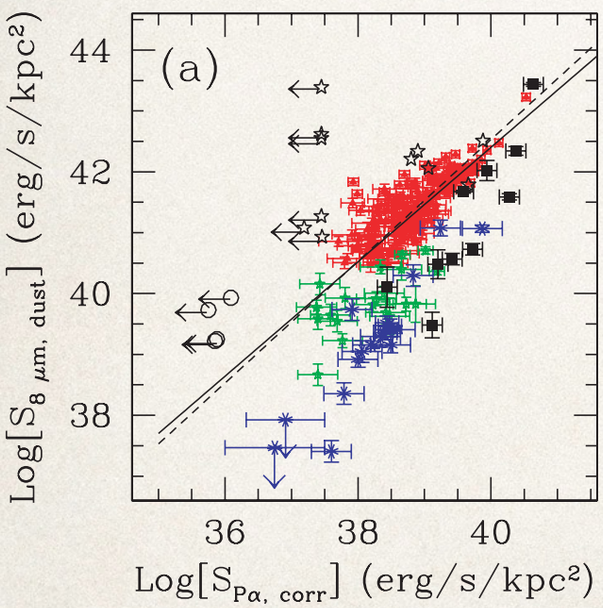

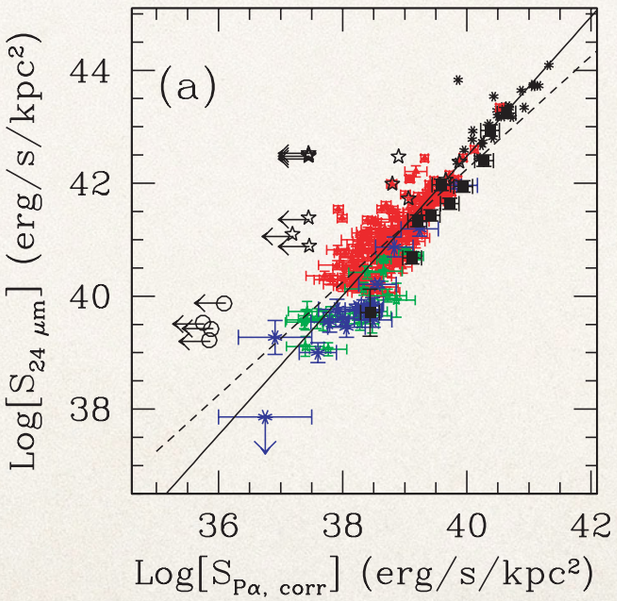

Calzetti+07

FIR-radio correlation

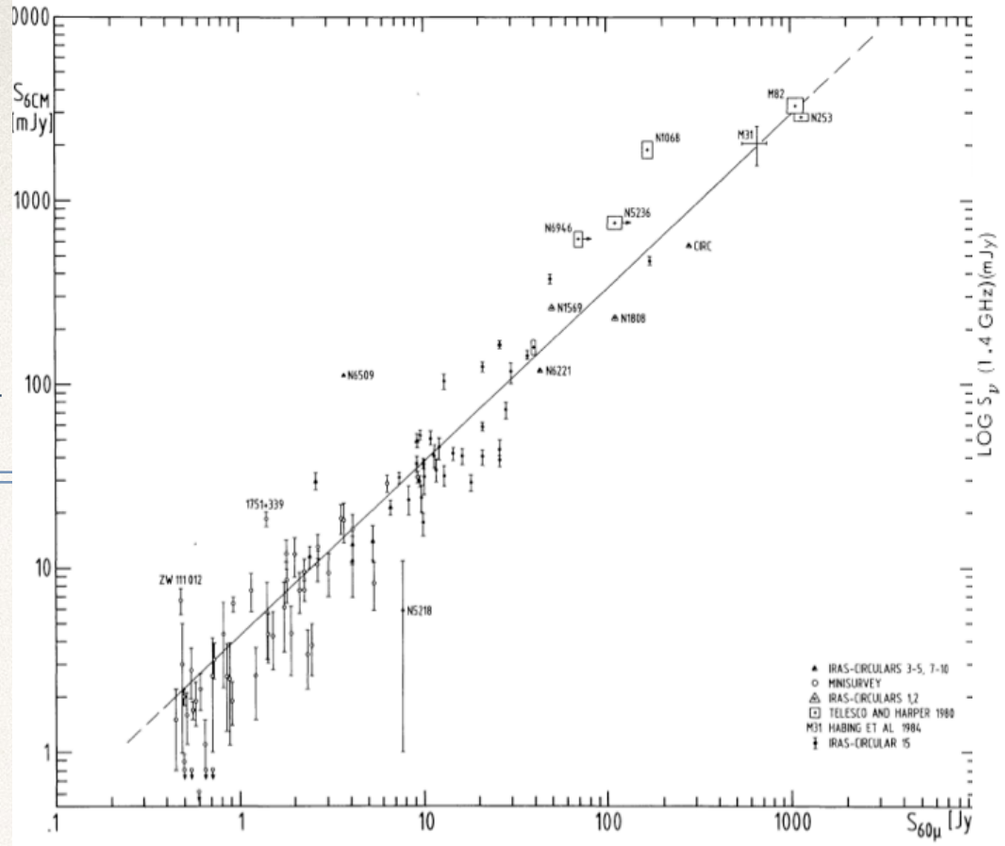

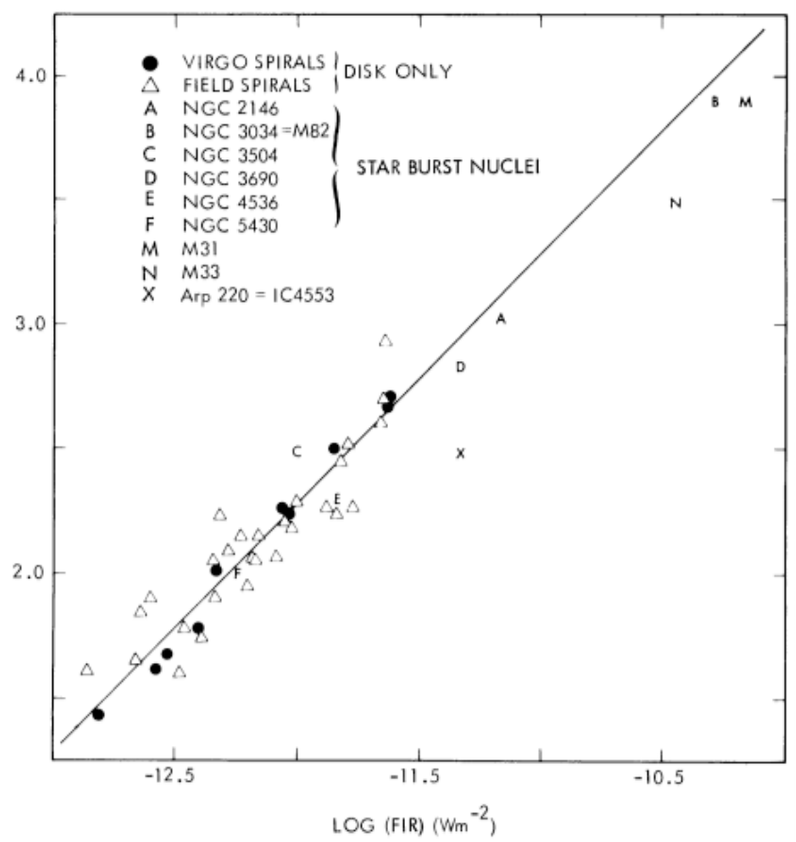

de Jong+1985; Helou+1985: GHz vs. 60μm or FIR

- $L_{FIR} \propto SFR$, FIR-radio correlation $\Rightarrow L_{GHz} \propto SFR$: why??
- GHz is synchrotron, i.e. relativistic CR electrons + magnetic field
- CR electrons are produced in SN explosions
- "Electron Calorimeter" theory: synchrotron cooling timescale shorter than the escape time: $t_{synch} << t_{escape}$ and synchrotron dominates (Völk 89; Lisenfeld+96)
- Reproducing the slope of the spectrum not trivial... need to work out many many details (see Lacky +10)

Bolometric SFR indicators: UV-IR

- Combine emerging UV flux with flux re-emitted in the IR by the dust

- Bell+05:

$$\frac{\psi}{M_\odot\ \mathrm{yr}^{-1}} = 9.8\times10^{-11}(L_{\mathrm{IR}} + 2.2L_{\mathrm{UV}})$$

SFR indicators

- Look up most updated references!
- Main review Kennicutt ARAA 1998
- Calzetti+07: mid-IR
- Calzetti+10: monochromatic FIR

Properties of the ionized gas

- See Osterbrock (1989)! Also review by Stasinska (2002, arXiv:astro-ph/0207500) - Dopita & Sutherland "Astrophysics of the Diffuse Universe"
- Key quantities:
  - T_e
  - n_e
  - abundances
- Key processes:
  - photon excitation and ionization
  - collisional excitation and de-excitation (electrons on atoms/ions)
  - recombination
  - radiative de-excitation

Ionized gas diagnostics

- Ionized ISM is optically thin to non-resonant lines (not so many atoms/ions excited above the ground state)

- Intensity of recombination lines almost independent of T, proportional to the number of recombinations, hence of ionizing photons if equilibrium holds

- Intensity of collisionally excited lines depends on T and n

- Resonant lines have very complicated behavior:

H Lyα, C IVλ1550, N Vλ1240, Mg IIλ2800

Gas (metallicity) diagnostics

- Use collisionally excited lines of atoms/ions of given element
  - O is the most popular, in fact estimates of gas metallicity are often given as 12+log(O/H), with solar [O/H] being 8.69
    - Forbidden lines: opposite to photon excited levels, collisionally excited levels do not require to follow the quantum selection rules relative to the ground state
- Dependence on density and temperature, not only element/ion abundance!
- "Direct" measurements require many lines, not always available for moderate SNR spectra
- Revert to indirect methods or "strong line methods"

Key concepts of collisionally excited lines
(see e.g. Dopita & Sutherland's book)

- Excitation rate depend on cross section
- Cross sections depends on the energy of the exciting electron (see figure)
- Energy of the electrons depends on temperature, following the Maxwell-Boltzmann distribution

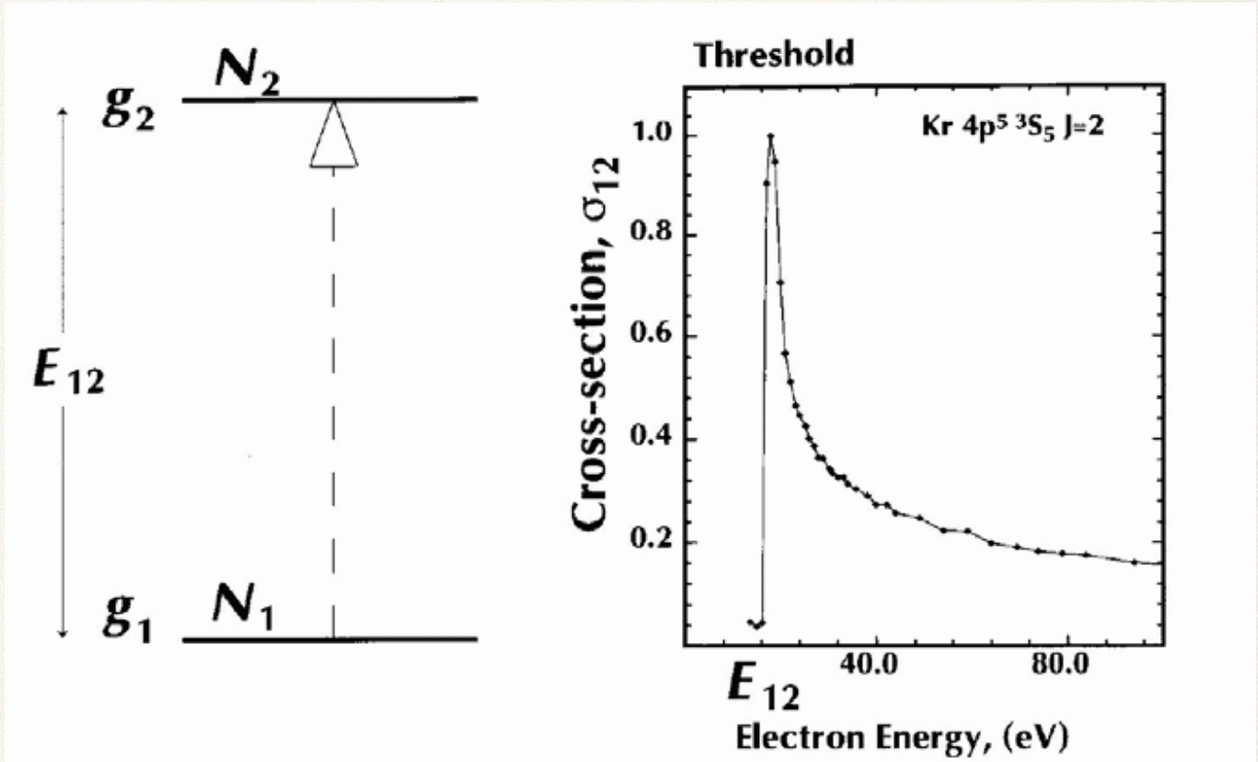

Fig. 3.1. Above the threshold energy for collisional excitation, the cross section decreases approximately inversely as energy (data from Chilton et al., 2000).

$$f_E(E) = 2\sqrt{\frac{E}{\pi}}\left(\frac{1}{kT}\right)^{3/2}\exp\left(\frac{-E}{kT}\right)$$

Collisional Rate $R_{12} \equiv n_e N_1 \alpha_{12} \equiv C_{12} N_1$:

$$R_{12} = n_e N_1 \int_{E_{12}}^{\infty} \sigma_{12}(E)\sqrt{\frac{2E}{m_e}} f(E)dE = n_e N_1 \left(\frac{2\pi\hbar^4}{km_e^3}\right)^{1/2} T^{-1/2}\left(\frac{\Omega_{12}}{g_1}\right)\exp\left(\frac{-E_{12}}{kT}\right)$$

V

Line emission of the two-level Atom

Low density limit: $R_{12} = C_{12} N_1 = N_2 A_{21}$ equilibrium set by radiative de-excitation rate

$$N_2 = n_e N_1 \frac{\alpha_{12}}{A_{21}} = n_e N_1 \left(\frac{2\pi\hbar^4}{k m_e^3}\right)^{1/2} A_{21}^{-1} T^{-1/2} \left(\frac{\Omega_{12}}{g_1}\right) \exp\left(\frac{-E_{12}}{kT}\right)$$

Emission line flux:

$$\mathrm{F}_{12} = E_{12} A_{21} N_2 = \chi_i n_e^2 \left(\frac{2\pi\hbar^4}{k m_e^3}\right)^{1/2} E_{12} T^{-1/2} \left(\frac{\Omega_{12}}{g_1}\right) \exp\left(\frac{-E_{12}}{kT}\right)$$

where $\chi_i = \mathrm{N_i}/\mathrm{n_e}$ is the relative abundance of the ion i considered.

For low temperatures the exponential term dominates because few electrons have energy above the threshold for collisional excitation, therefore the line rapidly fades with decreasing temperature. At high temperatures the $T^{-1/2}$ term controls the cooling rate, so the line fades slowly with temperature. The maximum line flux is reached at $T = E_{12}/k$.

To measure abundances χ_i one needs to know n_e and T_e.

Line emission of the two-level Atom

High density limit : Boltzmann equilibrium (LTE)

$$\frac{N_2}{N_1} = \frac{g_2}{g_1}\exp\left(\frac{-E_{12}}{kT}\right)$$

Emission line flux:

$$F_{12} = E_{12}A_{21}N_2 = \chi_i E_{12}A_{21}n_e\left(\frac{g_2}{g_1}\right)\exp\left(\frac{-E_{12}}{kT}\right)$$

Note that the line flux scales with n_e and it tends to a constant value at high temperatures.

Critical density where $A_{21} = R_{12}$:

$$n_{crit} = \left(\frac{A_{21}g_2T^{1/2}}{\Omega_{12}}\right)\left(\frac{2\pi\hbar^4}{km_e^3}\right)^{-1/2}$$ (see derivation in next slide!)

In a log n_e -log F plot the slope changes from 2 to 1 at this density.

Low density

$$\mathrm{F}_{12} = E_{12} A_{21} N_2 = \chi_i n_e^2 \left(\frac{2\pi\hbar^4}{k m_e^3} \right)^{1/2} E_{12} T^{-1/2} \left(\frac{\Omega_{12}}{g_1} \right) \exp\left(\frac{-E_{12}}{kT} \right)$$

$$=$$

$$\mathrm{F}_{12} = E_{12} A_{21} N_2 = \chi_i E_{12} A_{21} n_e \left(\frac{g_2}{g_1} \right) \exp\left(\frac{-E_{12}}{kT} \right)$$

High density

$$n_{crit} = \left(\frac{A_{21} g_2 T^{1/2}}{\Omega_{12}} \right) \left(\frac{2\pi\hbar^4}{k m_e^3} \right)^{-1/2}$$

Three-level Atoms, Ions with $E_{23} \ll E_{12}$

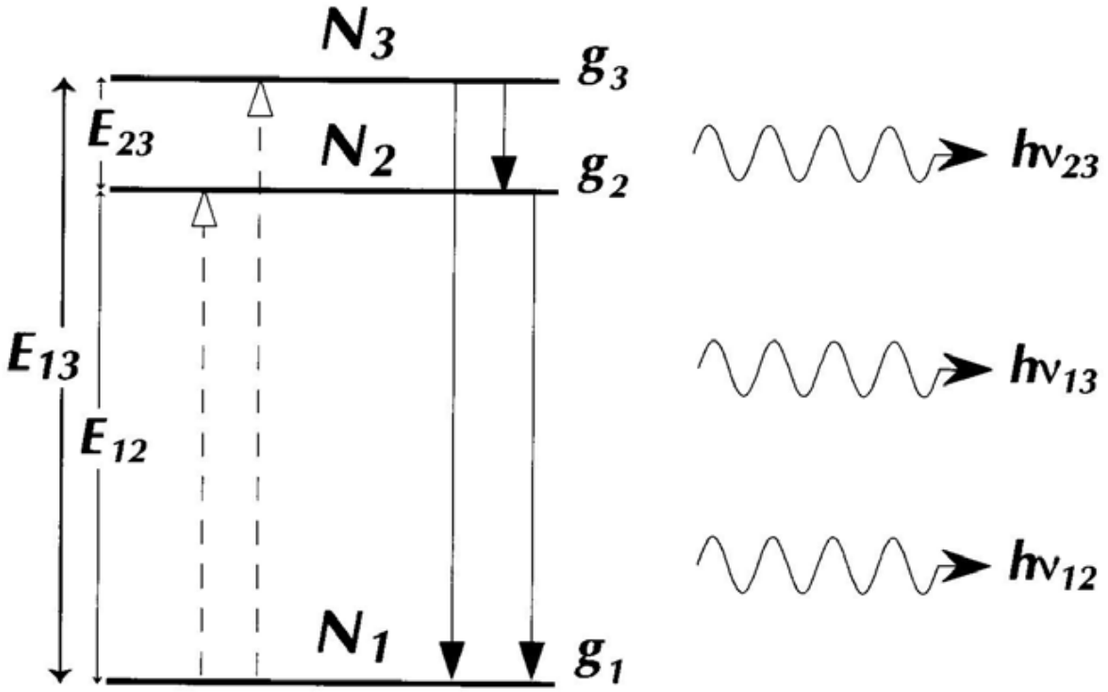

Fig. 3.5. An idealized three-level ion with a small energy separation between the excited states. Ions having configurations like this can be used for density diagnostic purposes.

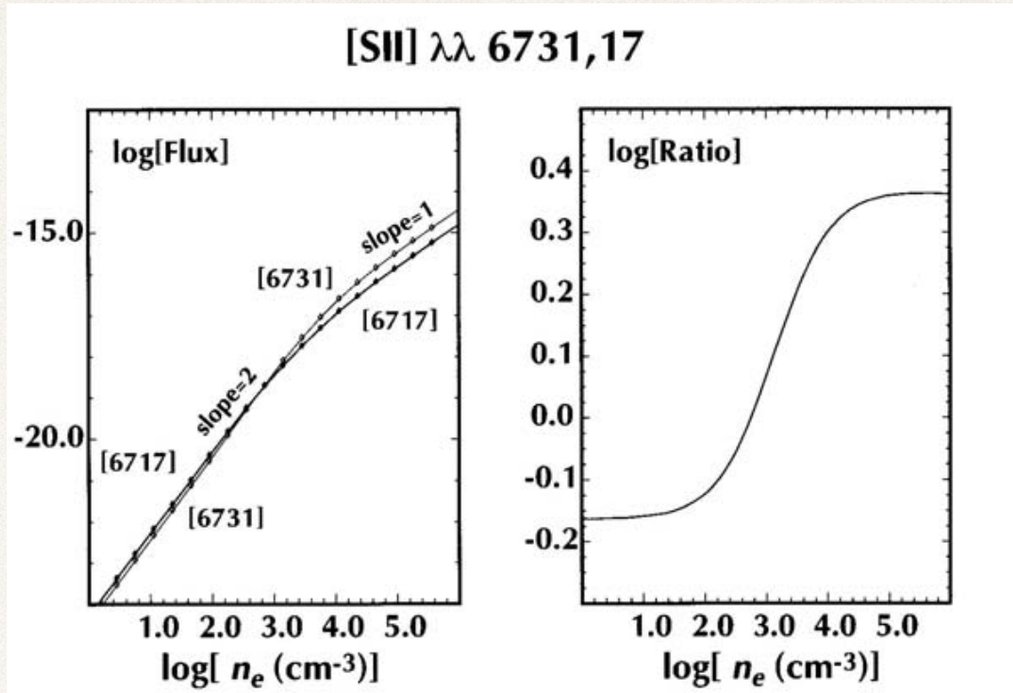

Fig. 3.6. The behavior of the emissivity (left) and the line ratio (right) as a function of density in the [S II] doublet which provides useful density diagnostics.

Low density limit: $C_{12}N_1 = N_2A_{21}, C_{13}N_1 = N_3A_{31}$

Flux ratio: $$\frac{F_{31}}{F_{21}} = \frac{E_{31}A_{31}N_3}{E_{21}A_{21}N_2} = \frac{E_{31}C_{13}}{E_{21}C_{12}} = \frac{\Omega_{31}}{\Omega_{21}}\exp\left(\frac{-E_{23}}{kT}\right) \approx \frac{g_3}{g_2}$$

Examples:
[OII]3726,3729
[SII]6731,6716
[ArIV]4740,4711

High density limit: Boltzman ratio $N_3 / N_2 = g_3 / g_2$

Flux ratio: $$\frac{F_{31}}{F_{21}} = \frac{A_{31}}{A_{21}}\frac{g_3}{g_2}$$

DENSITY INDICATOR

~1 Only if E_{23}/kT is small!

Key points for n_e determinations

- Same "ground" level of the same ion: remove the χ_i dependence
- $E_{32} << E_{31}$: remove the temperature dependence in the low density regime

Focus on Temperature

- Low density:

$$\mathrm{F}_{12} = E_{12} A_{21} N_2 = \chi_i n_e^2 \left(\frac{2\pi\hbar^4}{k m_e^3} \right)^{1/2} E_{12} T^{-1/2} \left(\frac{\Omega_{12}}{g_1} \right) \exp\left(\frac{-E_{12}}{kT} \right)$$

- High density:

$$\mathrm{F}_{12} = E_{12} A_{21} N_2 = \chi_i E_{12} A_{21} n_e \left(\frac{g_2}{g_1} \right) \exp\left(\frac{-E_{12}}{kT} \right)$$

Three-level Atoms, Ions with $E_{12} \approx E_{23}$

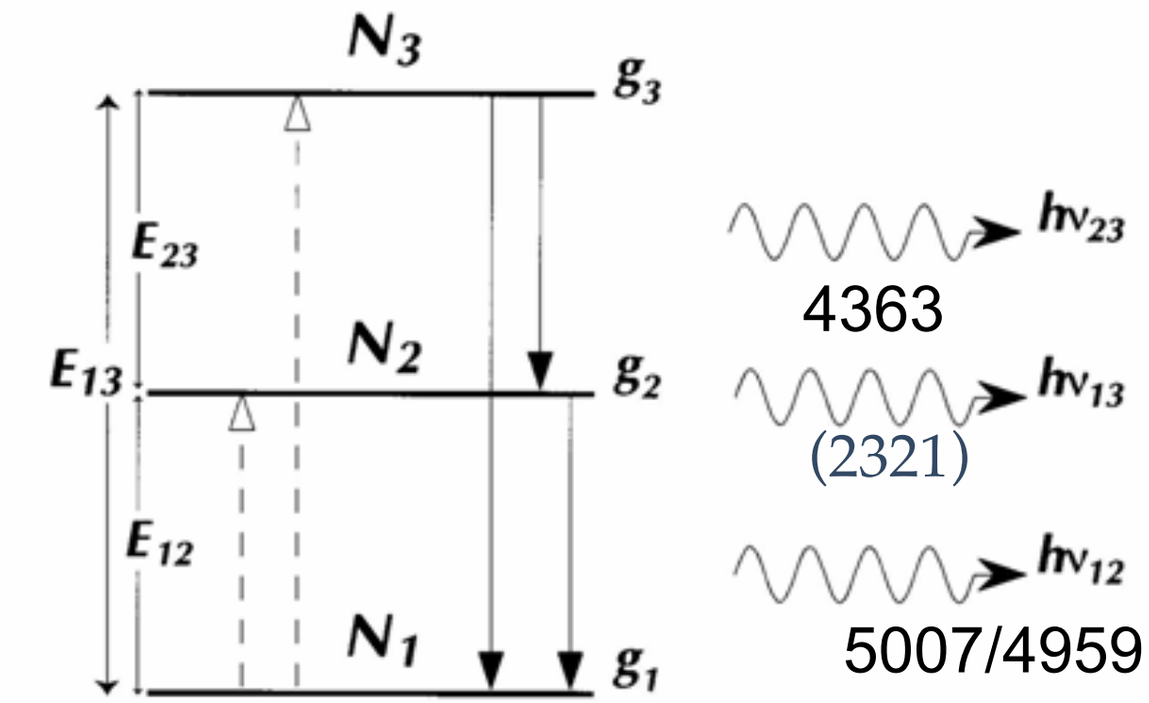

Fig. 3.3. A three-level atom with nearly equispaced excited states. Such a level configuration allows the ion to be used for temperature diagnostic purposes.

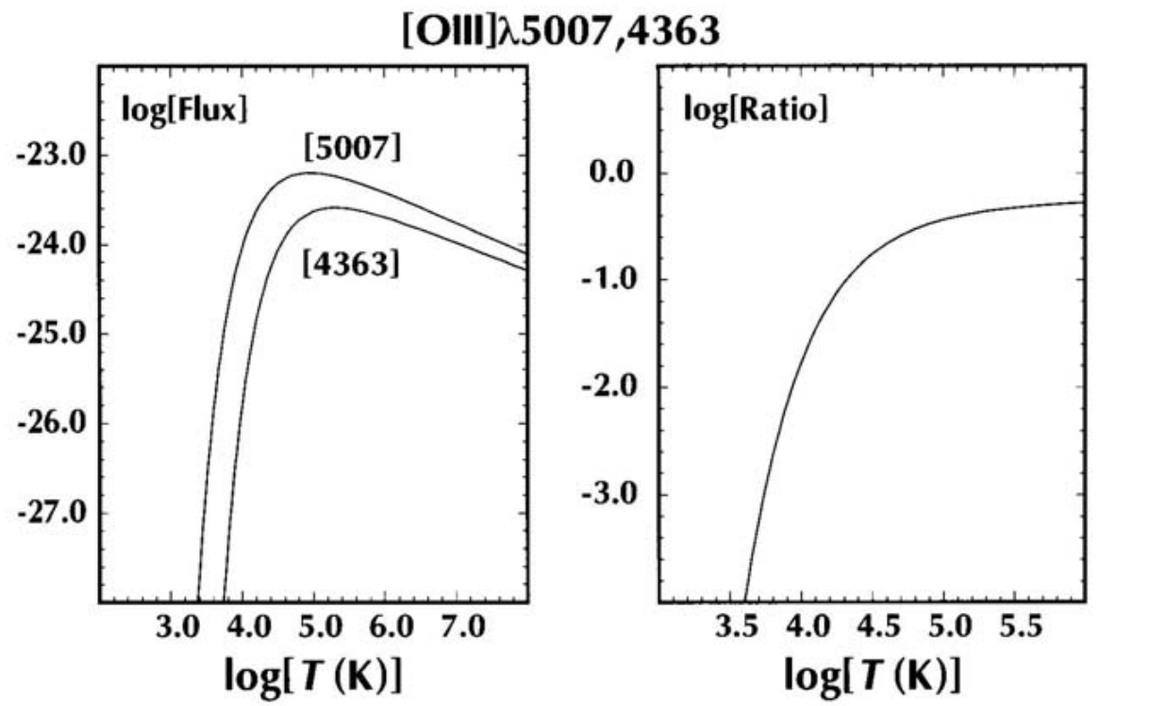

Fig. 3.4. The temperature dependence of the emissivity (left) and the ratio (right) of the two [O III] lines, λ 5007 Å and λ 4363 Å.

$$F_{12} = E_{12} A_{21} N_2 = \chi_i n_e^2 \left(\frac{2\pi\hbar^4}{k m_e^3}\right)^{1/2} E_{12} T^{-1/2} \left(\frac{\Omega_{12}}{g_1}\right) \exp\left(\frac{-E_{12}}{kT}\right)$$

Low densities:

$$N_1 C_{13} = N_3 (A_{32} + A_{31})$$
$$N_1 C_{12} + N_3 A_{32} = N_2 A_{21}$$

Normalization

$$N_1 + N_2 + N_3 = 1$$

Equilibrium: same total transition rates from/to levels

$$\frac{F_{32}}{F_{21}} \approx \frac{E_{32}}{E_{21}} \frac{C_{13}}{C_{12}} \frac{A_{32}}{A_{31}}$$

$$\frac{C_{13}}{C_{12}} = \frac{\Omega_{13}}{\Omega_{12}} \exp\left(\frac{-E_{23}}{kT}\right)$$

Examples:

[OIII]4363,5007/4959

[NII]5755,6583/6548

[SIII]6312,9532/9069

Flux ratio: $\frac{F_{32}}{F_{21}} = \frac{E_{32}}{E_{21}} \frac{A_{32}}{A_{31}} \frac{\Omega_{13}}{\Omega_{12}} \exp\left(\frac{-E_{32}}{kT}\right)$

TEMPERATURE INDICATOR

Key points for T_e determinations

- Same "ground" level of the same ion: remove the χ_i dependence
- $E_{32} \sim E_{21}$:
  - $C_{13} \ll C_{12}$
  - Emission lines at similar wavelengths
- Make sure the density is below the critical one, otherwise the low-density approximation does not apply

"Strong line methods"

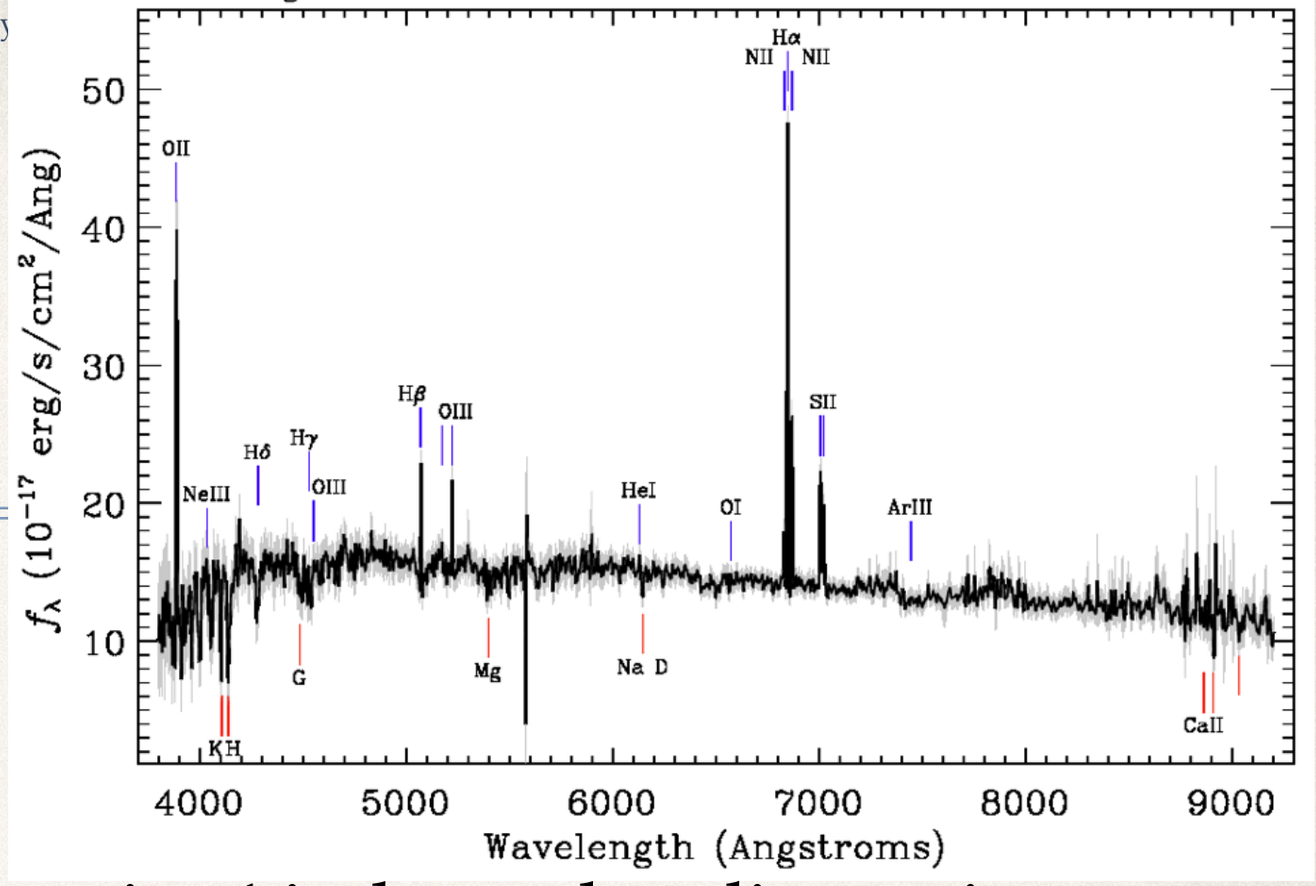

- n_e, T, abundance and extinction require 4 independent line ratios (sensitive to these quantities!)
- only 4 strong lines typically well measured (Pagel 1979): Hα, Hβ, [OII] λ3727 and [OIII] λ5007 $\Rightarrow$ 3 independent line ratios
- Hβ/Hα Balmer decrement $\Rightarrow$ extinction
- empirical dependence of T (and n_e) on metallicity
- Alternatively: simultaneous fit of several lines based on photoionization models (e.g. Tremonti et al. 2004)

R_{23} method

$$R_{23} = ([\mathrm{O\ II}]\ \lambda 3727 + [\mathrm{O\ III}]\ \lambda\lambda 4959, 5007)/\mathrm{H}\beta$$

- Two branches, high and low Z
- Requires calibration using direct methods
- needs a rough estimate of metallicity to choose the branch! other Z-sensitive line ratios must be adopted (see Kewley & Ellison 2008)

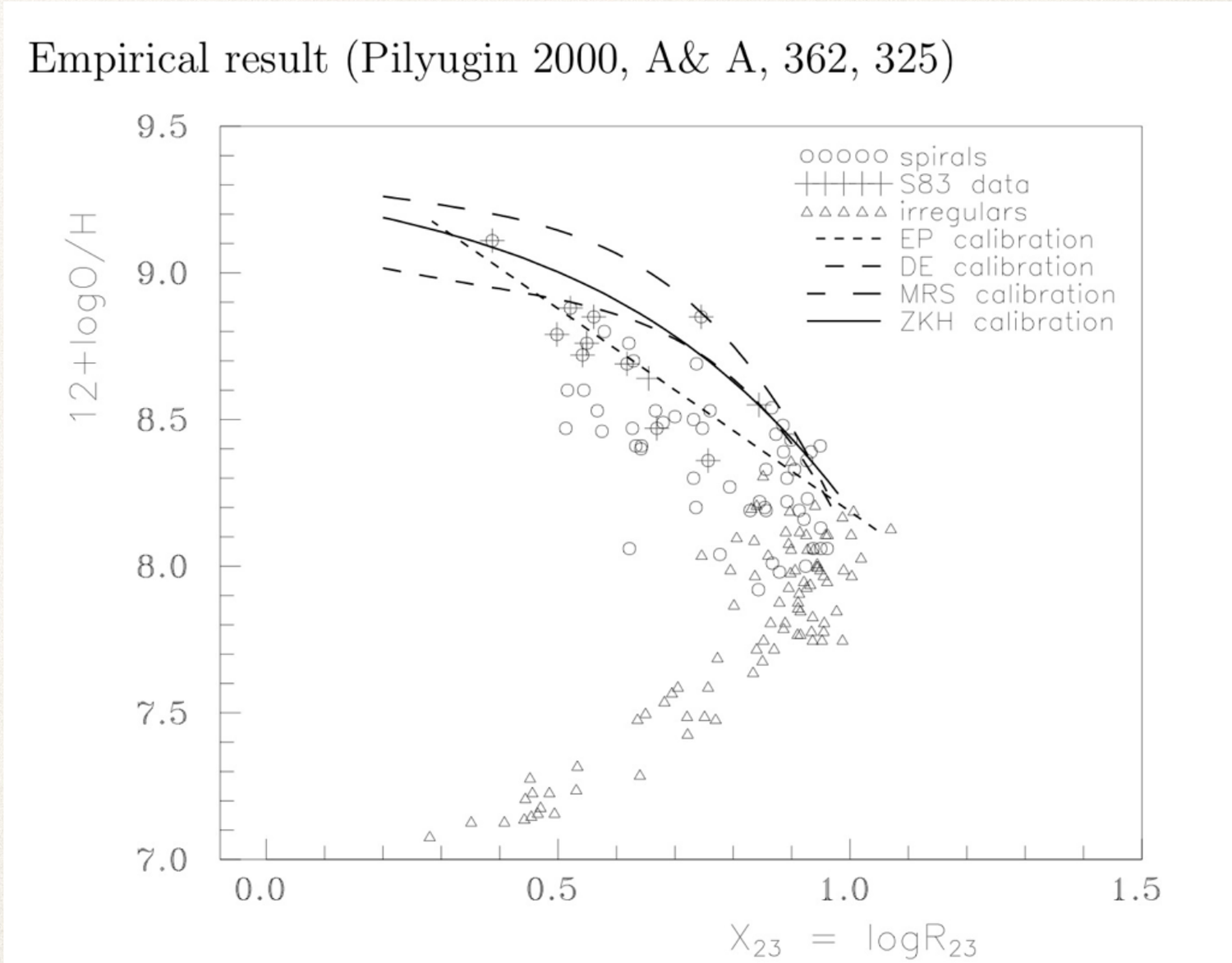

BPT diagram(s)

- Insensitive to reddening and absolute flux calibration
- Insight into heating mechanisms

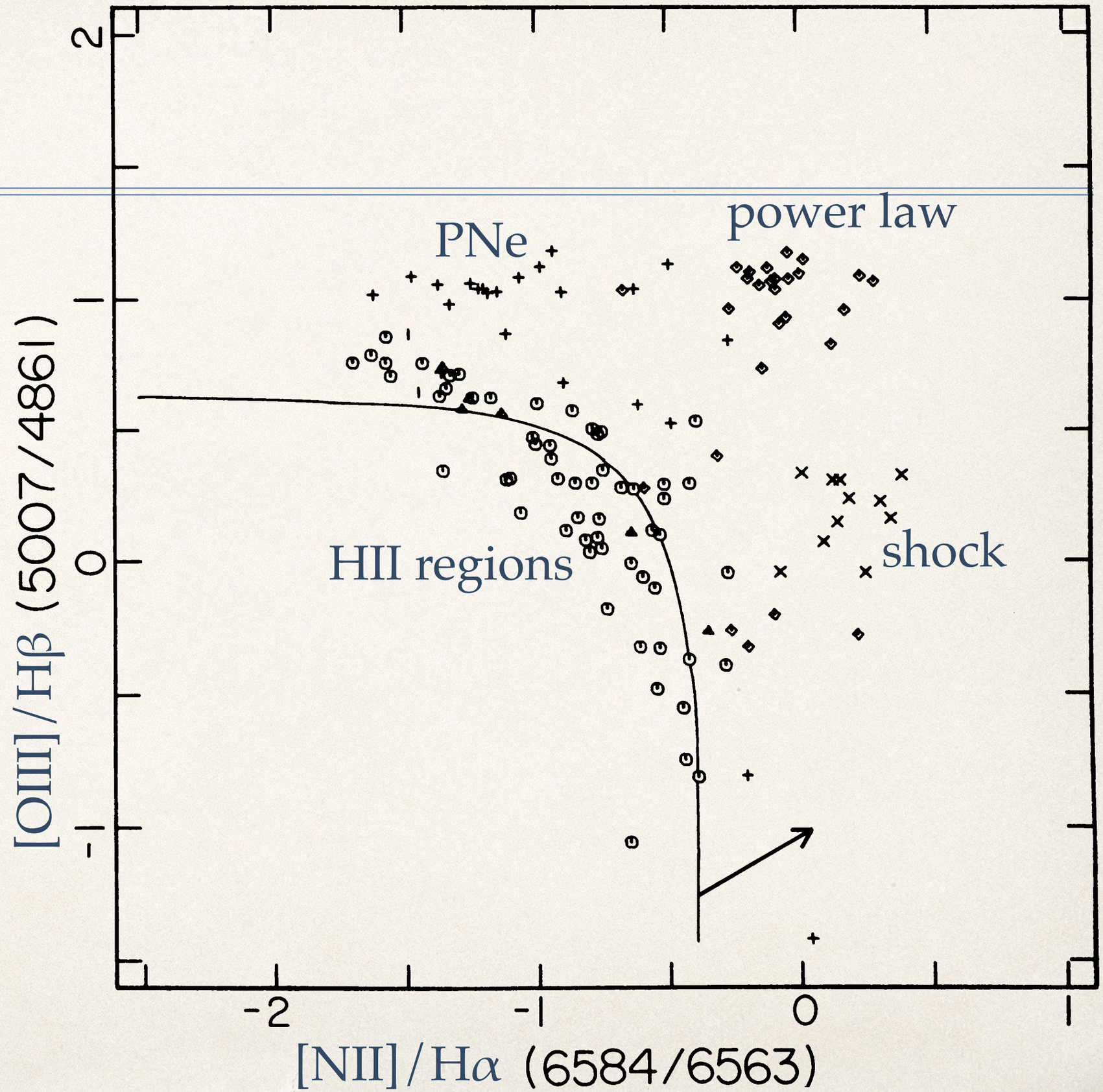

The physics of BPT diagrams

- Metallicity [O/H]
- Shape of the spectrum ("hardness")
- Ionization parameter of the radiation field: density of ionizing photons (Lyman continuum) over electron density

$$u = \frac{1}{4\pi r^2 N_e c} \int_{\nu_0}^{\infty} \frac{L_\nu}{h\nu} d\nu$$

$H + IE \rightarrow H^+ + e^-$	IE = 13.6 eV
$N + IE \rightarrow N^+ + e^-$	IE = 14.5341 eV
$O + IE \rightarrow O^+ + e^-$	IE = 13.6181 eV
$O^+ + IE \rightarrow O^{++} + e^-$	IE = 35.1185 eV

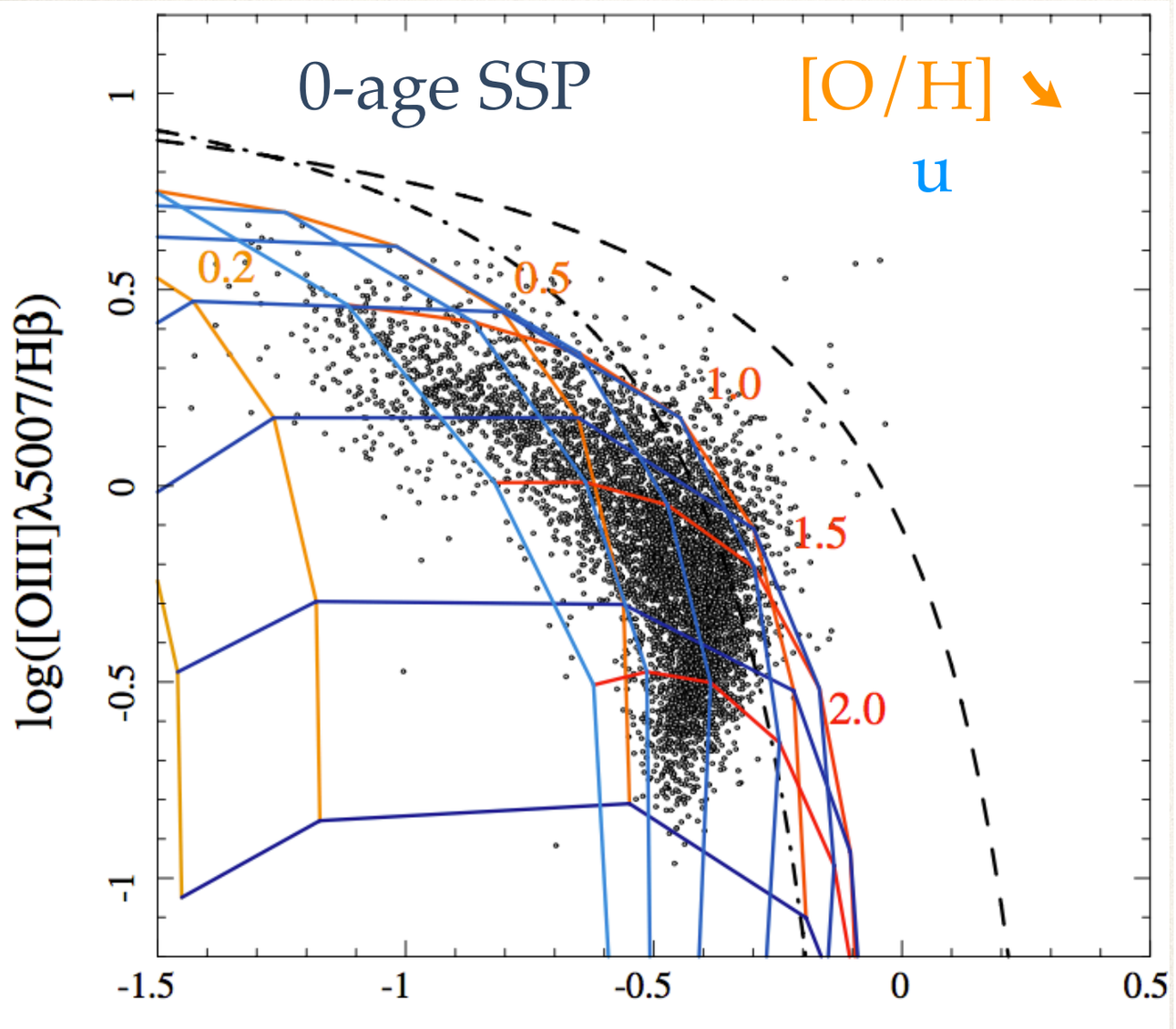

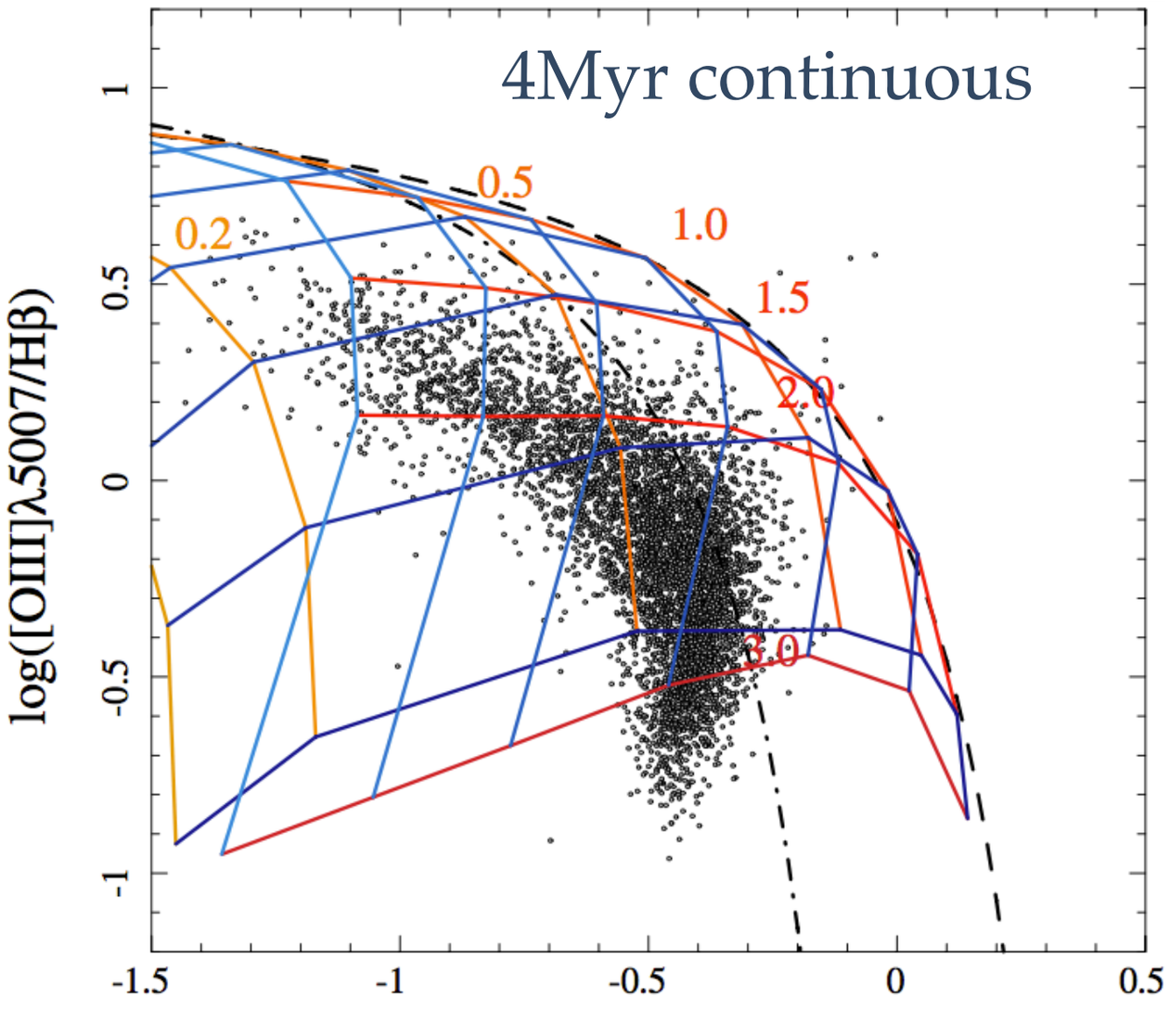

Sánchez+2015, CALIFA

The physics of BPT diagrams

- Metallicity [O/H]

- Electron density: increases rate of collisional excitation

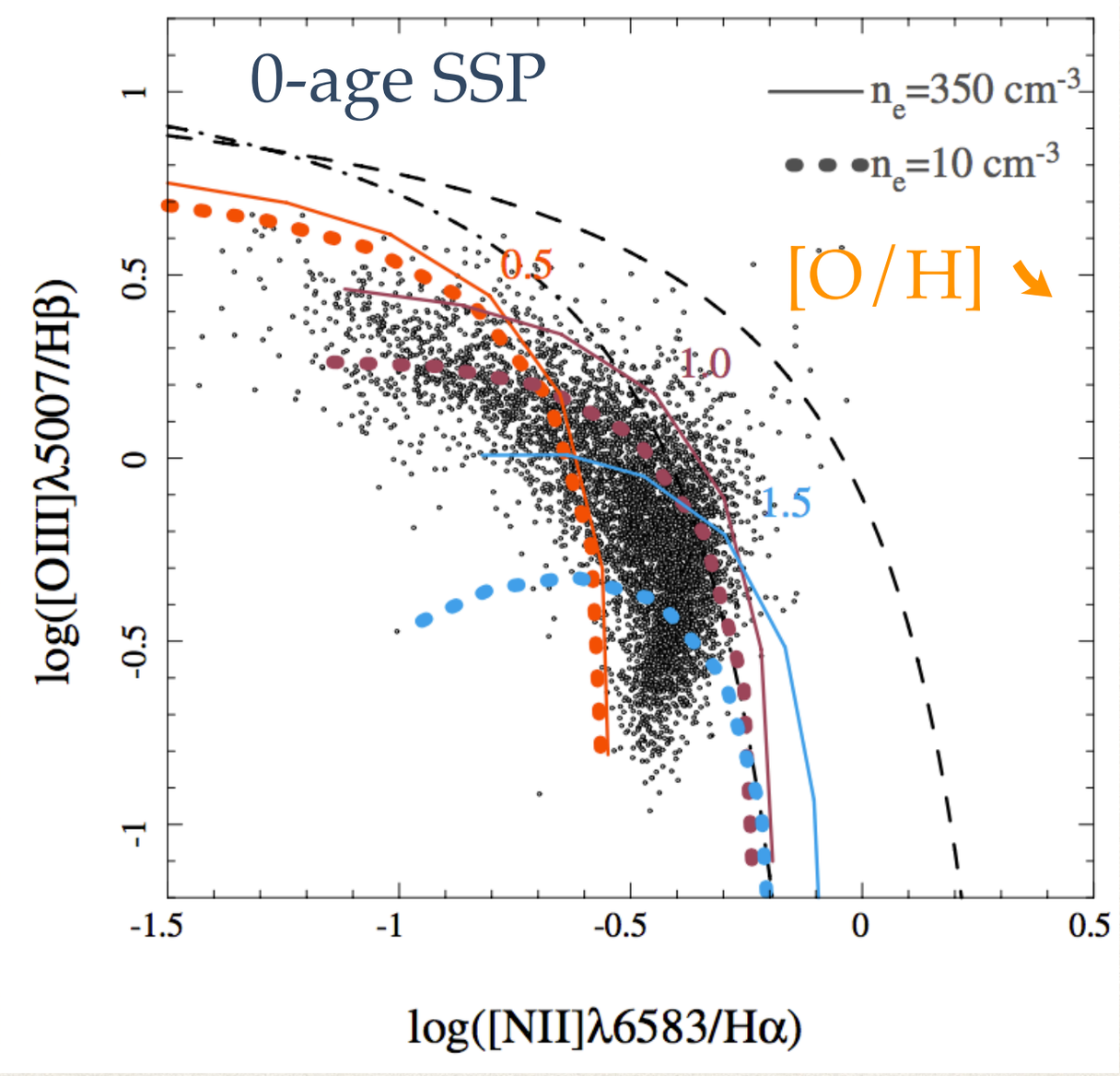

- Dust extinction

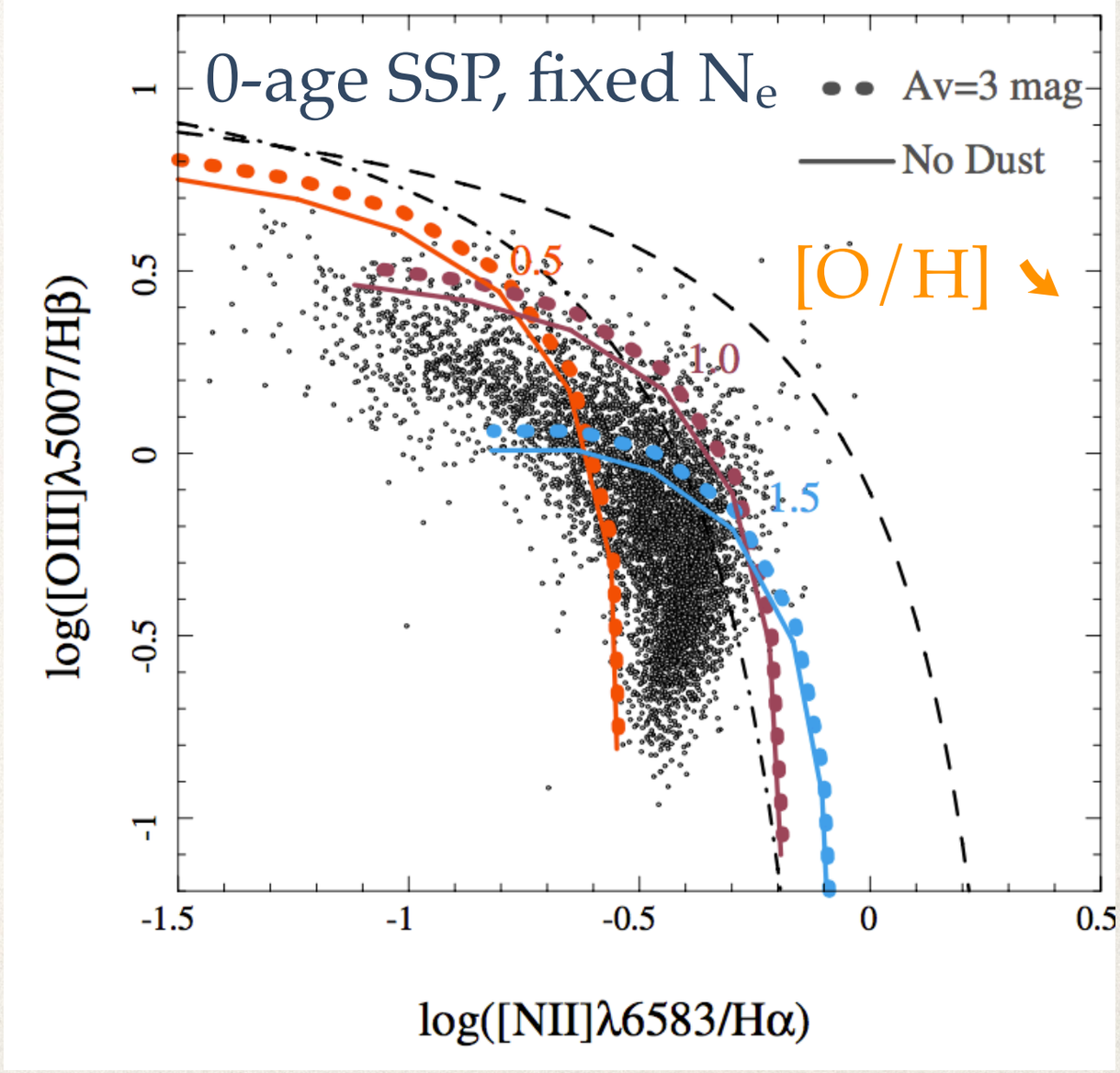

Sánchez+2015, CALIFA

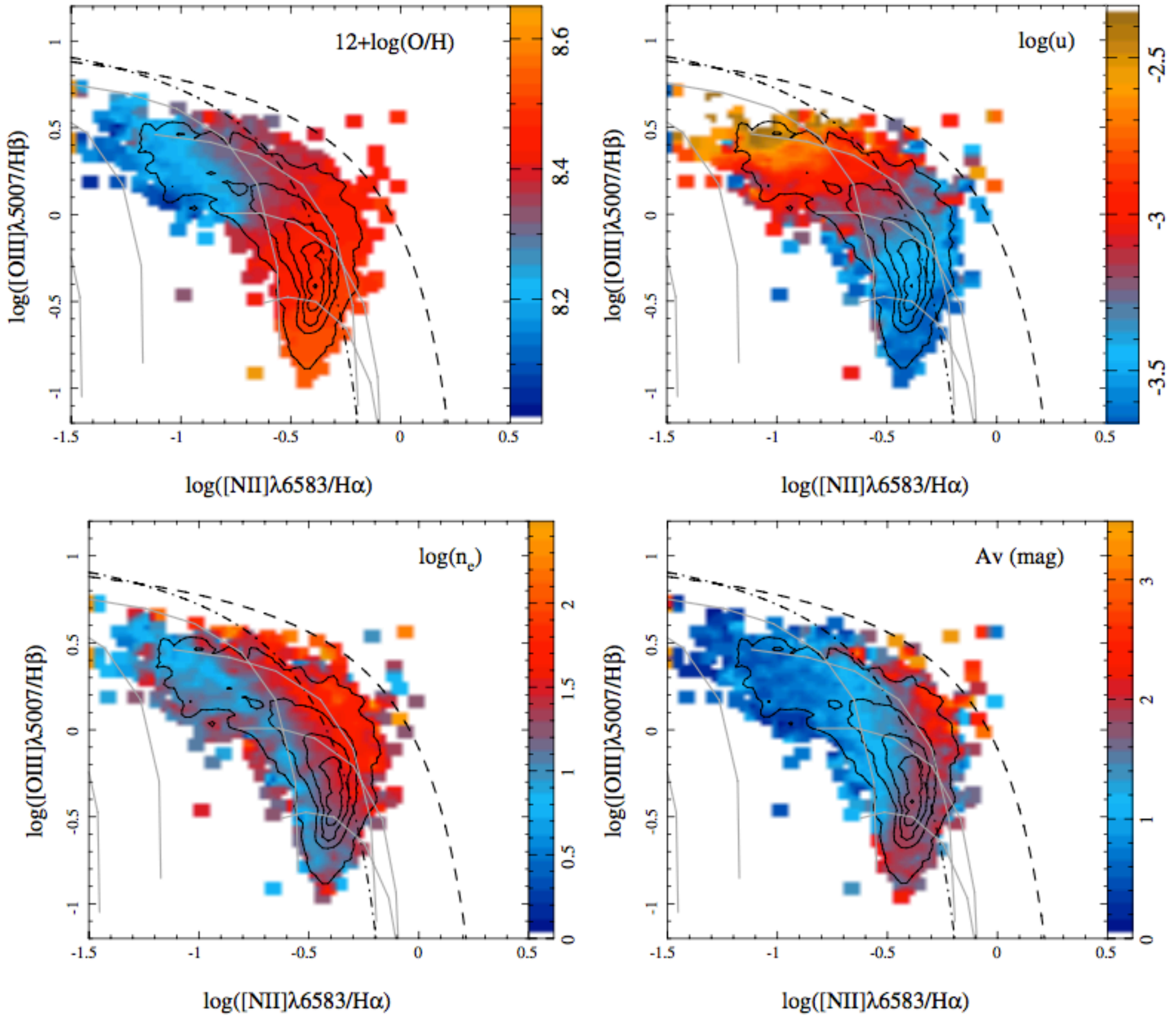

Fig. 2. [O III] λ5007/Hβ vs. [N II] λ6583/Hα diagnostic diagram for the ~5000 H II regions included in our sample. The contours show the density distribution of these regions within the diagram plane, with the outermost contour enclosing 95% of the regions and each consecutive one enclosing 20% fewer regions. In each panel the color indicates the average value at the corresponding location in the diagram for one of the four parameters

Sánchez+2015, CALIFA

BPT diagrams

- Emission line classification of galaxies: the role of the **AGN**!
- T-Z sequence for HII galaxies in [NII] BPT
- Radiation "hardness" and shocks diagnostics to the right of the line

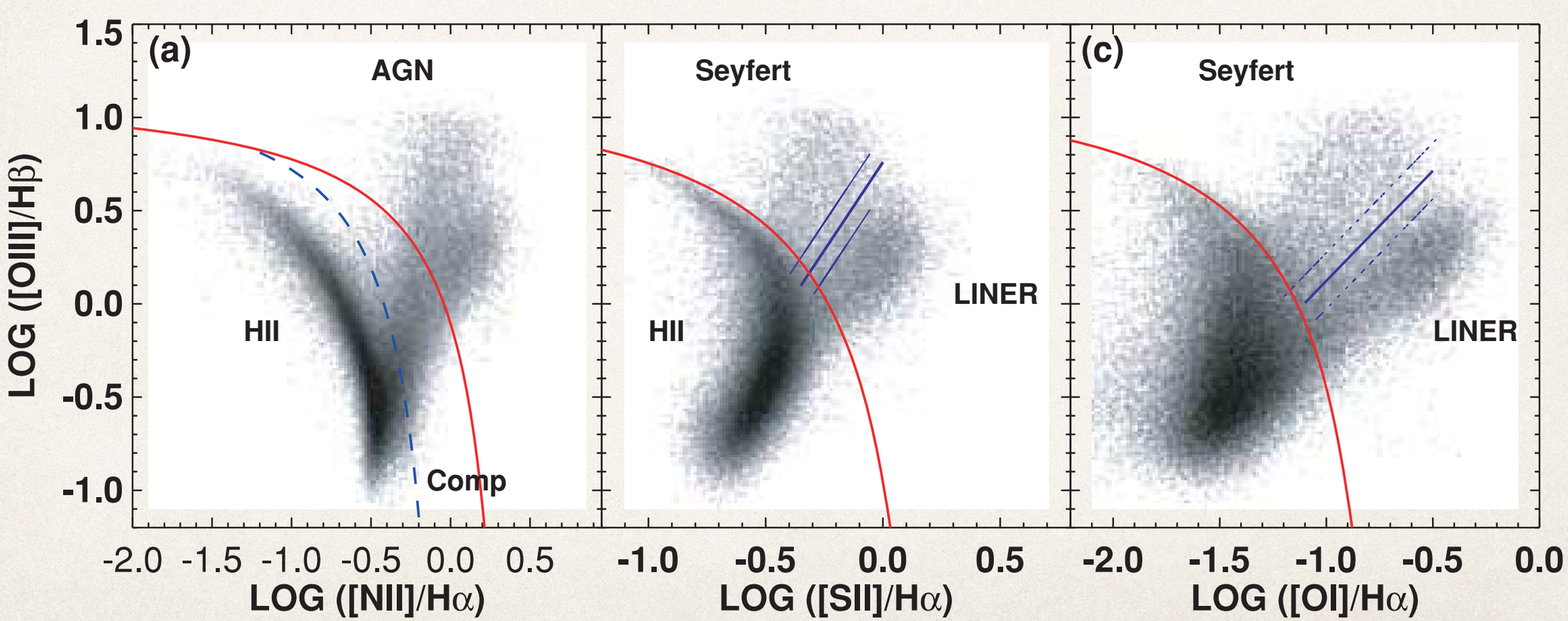

Kewley et al. (2006) [also Kauffmann et al. 2003]

Emission lines from AGN

- Type I:
  - Broad permitted lines directly from BLRs (Balmer lines, MgII, CIV, Lyα)
    - FWHM>2000 km/s
  - Narrow forbidden lines from NLRs ([OIII], [NII], [OII] etc.)
- Type II:
  - narrow permitted and forbidden lines, FWHM ~ several 100 km/s
- Possible mixing with emission from HII regions and diffuse ionized gas